ESTIMATING THE NET SURFACE SHORTWAVE RADIATION USING MODIS DATA

S.M.J.S.SAMARASINGHE
February, 2014

SUPERVISORS:
Dr. Ali A. Abkar
Dr. Valentyn A. Tolpekin

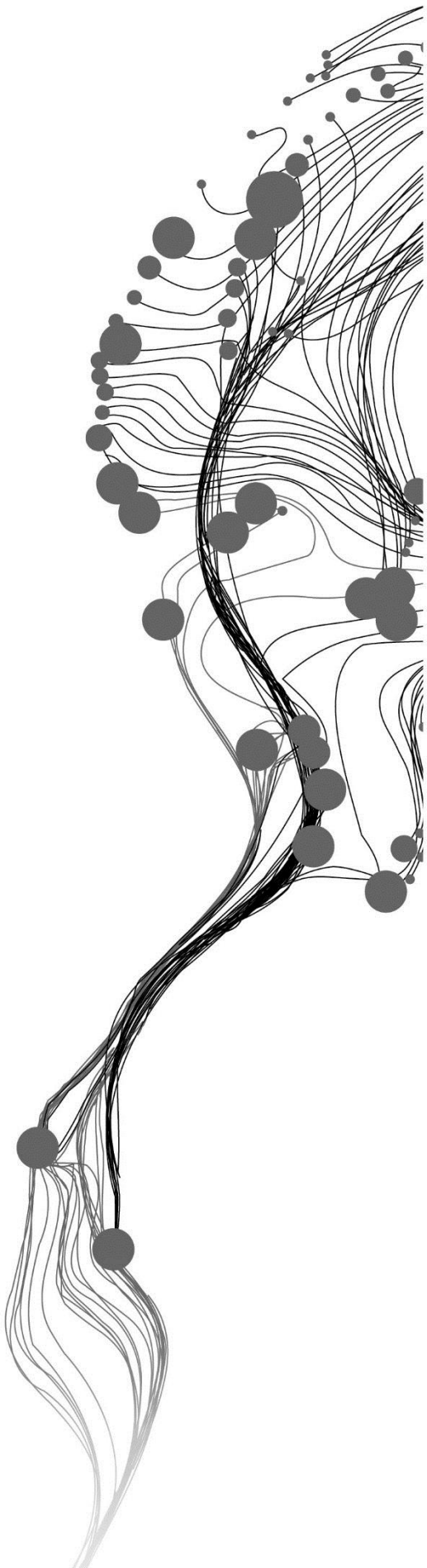

ESTIMATING THE NET SURFACE SHORTWAVE RADIATION USING MODIS DATA

S.M.J.S.SAMARASINGHE

Enschede, The Netherlands, February, 2014

Thesis submitted to the Faculty of Geo-Information Science and Earth Observation of the University of Twente, The Netherlands and K.N.Toosi University of technology (KNTU), Tehran, Iran in partial fulfilment of the requirements for the degree of Master of Science in Geo-information Science and Earth Observation.
Specialization: Geoinformatics.

SUPERVISORS:
KNTU Supervisor: Dr. Ali A. Abkar
ITC Supervisor: Dr. Valentyn A. Tolpekin

THESIS ASSESSMENT BOARD:
Prof. G. Vosselman, (ITC) (Chair)
Dr. M.R. Sahebi (External Examiner)

FACULTY OF GEO-INFORMATION SCIENCE AND EARTH OBSERVATION (ITC) OF UNIVERSITY OF TWENTE, ENSCHEDE, THE NETHERLANDS, &
KN TOOSI UNIVERSITY OF TECHNOLOGY, TEHRAN, IRAN

THIS THESIS IS DEDICATED TO:

FIRST AND FOREMOST TO RESPECT MY MOTHER AND FATHER, SECONDLY, MY EVER SUPPORTIVE LOVING SON RUMETH AND WIFE LALANI.

ABSTRACT

Net Surface Shortwave Radiation (NSSR) is a key quantity for the estimation of net radiation(R_n), and R_n is a key component of the Earth energy balance and is used for various applications including climate monitoring, weather prediction and solar power generation. The most practical and reliable method for estimating solar radiation is based on remote sensing because remote sensing observation values are higher than location based measurements for acquiring the features of global coverage (Liang et al., 2012).

Over the past years, many models for estimating surface shortwave radiation or its components have been developed from various remote sensing observations by combining remote sensing observations with ancillary surface and atmospheric data.

It has been observed that existing ancillary data are not sufficient to have an accurate solar radiation estimates due to the limited amount of ground equipment and calibration and maintenance processes hence available net surface shortwave solar radiation data is not accurate. Therefore, in this research the aim is to fill this gap and provide the required information on reliable spatial solar radiation data to the user community using high spatial and temporal resolution remote sensing data and products.

This research tries to provide accurate solar radiation data based on the data and products from Moderate Resolution Imaging Spectroradiometer (MODIS), on board the Earth Observing System (EOS) Terra satellite, as an alternative solution for existing unreliable pyranometer data.

The primary objective of this research is to explore an appropriate methodology to capture the spatial distribution of NSSR using MODIS data, which is more suitable for use in Iran. In addition, this study describes the methods for estimating instantaneous and daily average NSSR using different algorithms. Since instantaneous NSSR estimates have limited usage compared to daily average net radiation values (DANR), hence a sinusoidal model is applied to estimate DANR with estimated accurate day length.

By this developed model with initial parameters, the average RMSE value for estimated instantaneous NSSR is 29.44 W m^{-2}, 55.51 W m^{-2} and 44.43 W m^{-2} for the clear sky, cloudy sky and both clear and cloudy sky condition respectively. For the estimated daily average NSSR, value of average RMSE is 29.53 W m^{-2}, 31.83 W m^{-2} and 30.70 W m^{-2} for the clear sky, cloudy sky and both clear and cloudy sky condition respectively. Lastly Instantaneous NSSR and Daily average NSSR also mapped over the study area.

ACKNOWLEDGEMENTS

The writing of this thesis has been one of the most challenging yet interesting academic enterprise that I have ever had to involve myself. Without the support, patience and guidance of the following individuals, this study would not have been completed. It is a pleasant aspect that I have now the opportunity to express my gratitude.

The person to whom I am most indebted is Dr. Ali A. Abkar, KNTU supervisor who became my dear friend. I must confess that this thesis owes much of its existence to Dr Abkar, who inspired me whenever I needed it while dealing with many exhausting issues. He helped me in fine tuning the thesis topic and clarifying the intricacies. With great patience and energy, Dr. Abkar guided me in the right direction in this long journey, instructing and help organizing my thoughts and clothing them in appropriate words. Without his support and encouragement, the journey of my thesis writing may never have ended up in success.

I would like to gratefully and sincerely thank Professor Dr. Valentyn A. Tolpekin, ITC supervisor for his guidance, understanding, patience, and most importantly, the trust he placed in me during my studies at ITC. His mentorship was paramount in providing a well-rounded experience that is consistent with my long-term career goals.

I would like to express my deepest appreciation of the committee chair Professor Prof. G. Vosselman, (ITC) who demonstrated the attitude and the substance of a genius who continually and persuasively imputed that spirit of adventure in regard to research. Without his advice and constant help this thesis would not have been possible. At the same time I wish to thank to Professor Dr. Kourosh Khoshelham, course coordinator ITC, whose continued concern was always an encouragement.

My appreciation is incomplete, if I do not mention the support and help extended by Professor Dr. Mashhadi Hossainali, Faculty of Geodesy and Geomatic Engineering, KNTU, by means of valuable suggestions, inherent views on research and encouragement and also caring about my living environment. I consider it an honor to work with him.

I praise the enormous amount of help and teaching by Dr. Ali Mohammad Zadeh, Dr. Reza Malek, Dr. Asghar Ale Sheikh, Dr. Mohammad Mesgari and Dr. Ali Mohammadi. For this thesis I would like to thank Dr. Gamini Wickramasinghe and his wife Subha for their time, interest, and helpful comments.

At the same time, I wish to express my thanks to Professor, Chris A. Gueymard, Solar Consulting Services, USA and Dr. Damien Garcia, University of Montreal Hospital, Canada for their assistance during the experiments and helpful discussions.

I am indebted to many of my colleagues who interacted with me in my work. In Iran and in The Netherlands, Medhi, Aki, Poyam and Azar proved their value as helpful and caring class mates, and I share the credit of my work with Miss: Mojgan Mirzaie, for her support for the development of codes, and Hussain, Nabi, Vahid and Islam, doctoral students, for their support for the thesis improvements.

This thesis would not have been possible if not for the support and encouragement by the officers of the Faculty of Geo-information Science and Earth Observation (ITC) of University of Twente, Netherlands and KN Toosi University of Technology, Tehran, Iran and Survey Department of Sri Lanka specially Mrs. ALSC Perera, Deputy Surveyor General (LIS/GIS) and Mr S.Sivanantharajah, Senior Supdt of Surveys (GIS), I am indebted to them for their precious help.

Furthermore, I would like to give my warmest thanks to the respectable organizations for their valuable and unconditional help to develop this research.
I owe a debt of great magnitude to NUFFIC that generously funded this research in addition to providing the opportunity to meet many interesting and educated personalities.
This study has been conducted as part of the Iranian Space Agency (ISA) research program No. 91/900/920/3113 "Estimation of daily solar radiation using MODIS data". Therefore, all data and rights belong to the ISA.
Finally, it is the enduring and unconditional help, sharing and caring that I received from my wife and child who willingly sacrificed a great deal that enabled me to remain oriented to the studies and eventually gain these achievements; I would fail in my duty if I do not openly acknowledge their support and understanding. It will always remain uppermost in my cherished memory.
.

TABLE OF CONTENTS

LIST OF FIGURES

LIST OF TABLES

1. INTRODUCTION

1.1. Motivation and problem statement

Model evaluations and development for estimation of instantaneous incoming shortwave solar radiation over an area using satellite images is very essential in order to study the effects of solar radiation on the Earth system. The incident shortwave solar radiation, also known as insolation, is referred to as the total solar irradiance incident at Earth surface. Solar energy has come into widespread use where other power supplies are absent, such as in remote locations and in space. As a result the need for solar radiation data became more and more important and estimating solar irradiation incident on surfaces for estimating climate variables and building energy efficiency in the solar energy industry.

Conventional energy sources based on oil, coal, and natural gas are reducing day by day and damaging economic systems, environment and human life. Renewable energy sources such as solar can provide sustainable energy services based on the availability. Therefore availability of solar radiation for community through the solar panel systems, may reduce the decreasing rate of available fossil fuel quantity as well as reduce the cost of energy usage.

Solar irradiance is the amount of solar energy that arrives at a specific area at a specific time. The average annual daily solar irradiation varies with a location and it is a good indicator about the location to establish solar panels. Hence there should be some references to identification of suitable location availability for solar potential. To answer such requirements, accurate spatial solar radiation data at high spatial and temporal resolution are needed. Remote sensing provides large volume of data referring to the land and atmospheric states. Reliability of the derived values from remote sensing data depends on the physical variables such as surface and air temperature, air emissivity and land surface albedo (Hwang et al., 2012), and the main factors that directly influence solar irradiation within the Earth's atmosphere are ozone, air molecules, aerosols, water vapour, clouds, geographical location, season and time of day (Dekker et al., 2012). The solar irradiance at some point reduced by the clouds, which have the effect of blocking the solar ray's thus limiting them from reaching the atmosphere (Schillings et al., 2004).
With this kind of situation many attempts have been made to estimate the net radiation (R_n) which equals the difference between the incoming and outgoing radiation of both short and long wavelengths from satellite observed radiance at different scales. Results being produced for such an approaches, neglecting the characteristics of spatial heterogeneity considered as a major drawback (Bisht et al., 2005).

Numerous attempts have been made to deliver calculation of instantaneous net radiation or its components by combination of advance satellite technology and available ground observed data. Hybrid algorithm method developed by Kim and Liang (2010) for both clear and cloudy sky using MODIS (Moderate Resolution Imaging Spectroradiometer) data, but the authors have mentioned that uncertainty in the model causes effect of the atmospheric heterogeneity. By presenting their solutions, Bisht and Bras (2010), Bisht and Bras (2011), Hwang et al. (2012) and Tianxing et al. (2012) have shown that studies developed different models to calculate net radiation for clear sky conditions, but development of accurate models for cloudy sky conditions still remains a significant challenge.

Today, the primary source of solar radiation data for Iran comes from measurements made by the Iranian Meteorological Organization using Pyranometer stations. Because of the limited amount of ground equipment and calibration and maintenance processes that they must go through, at least once a year, they do not always accurately measure the incoming solar radiation. Therefore, in this research the plan is to fill this gap and provide the required information on reliable spatial solar radiation data to the user community using high spatial and temporal resolution remote sensing images.

1.2. Research identification

The many data products derived from MODIS observations describe features of the land, and the atmosphere that can be used for studies of processes. The MODIS sensor has higher spectral, spatial, and radiometric resolutions, compared to previous sensor systems such as NOAA Advanced Very High Resolution Radiometer (AVHRR) sensor. MODIS instrument has a 12-bit radiometric resolution and an optimized onboard calibration subsystem that ensures high calibration accuracy (Guenther et al., 1998). The MODIS cloud mask algorithm by Ackerman et al. (2006) employs an automated threshold-based approach to identify clouds and these algorithms primarily use to label pixels as cloudy or clear.

Previous studies have developed remote sensing based land surface parameterization methods to estimate net radiation or its components using various kinds of satellite data at various scales. They explicitly recognized the need for spatially varying parameters to estimate downward shortwave radiation. The performance of the clear and cloudy sky condition model depends on the physical soundness of its parameterizations, and their ability to deal properly with utmost values of the main inputs.

A simple scheme developed by Bisht et al. (2005) to estimate instantaneous net radiation for clear sky days using remote sensing observations and eliminate the need for ground information as model input. Cloud cover represents the greatest potential losses in solar radiation within the Earth's atmosphere. Land surface framework have been developed by Bisht and Bras (2010) to estimate instantaneous net radiation for all sky conditions using remote sensing data. In above mentioned research, instantaneous net radiation was estimated using various Terra-MODIS land products such as MOD43 and MOD07 (land surface temperature, land surface emissivity, and land surface albedo) and Terra-MODIS atmospheric data products (air temperature, dew temperature, water vapour and aerosol depth). But this, MOD43 products consist of data gaps and considerable missing pixels (Huang et al., 2012).

Remote sensing based method was developed by Tang et al. (2006) to calculate Net Surface Shortwave Radiation (NSSR) at a 1 km resolution using MODIS data. In this method, narrowband to broadband albedo conversion, at the Top of Atmosphere (TOA) relation with narrowband apparent reflectance to shortwave broadband albedo for both clear and cloudy skies was developed. Results showed that this method could predict TOA shortwave broadband albedo accurately and coefficients have arranged by land surfaces, ocean surface and snow/ice surfaces. Estimated Net Surface Shortwave Radiation (NSSR) from MODIS data was compared with the available meteorological data (coefficient values and model accuracies are described in Chapter 7).

The core part of this algorithm based on Li's parameterization, Li et al. (1993a), Li. et al. (1993b) and Masuda et al. (1995). Recently developed four models including this Tang model to estimate NSSR in Eastern and Western China have evaluated by Huang et al. (2012) and described that calculated NSSR have slightly overestimated and linear coefficient (R^2) high, the accuracy is not as high as mentioned in Tang et al. (2006), whereas the other two hybrid algorithms (Albedo-Based Hybrid Algorithm-ABHA and Direct-Estimate Hybrid Algorithm-DEHA) have shown lower accuracy.

As observed by Nightingale et al. (2009), some Terra MODIS data and products have data gaps and missing pixels due to instrumentation errors, losses of image data during transmissions and atmospheric disturbances, therefore possibility to reduce data retrieval quality and result in periods of missing data. Tang et al. (2006), produced NSSR using Terra MOD05, NIR products and there are no data gaps except for band stripping errors (image noise).

This proposed study aims to evaluate and investigates the significance relationship of NIR precipitable water vapour amount and Solar Zenith Angle (SZA) in the model algorithm to calculate NSSR mentioned in Tang et al. (2006), algorithm derived from MODIS products for clear and cloudy sky conditions. The generation of instantaneous and daily NSSR will be the challenging part in this thesis.

1.2.1. Research objective

The magnitude and distribution of incoming shortwave solar radiation has significant influence on the productive capacity of solar energy related applications. Those applications require accurate and spatially available radiation surfaces. It helps to resolve or reduce uncertainty of their fundamental inputs for those applications. Therefore, in this research the objective is to provide spatial solar radiation maps using high spatial and temporal resolution MODIS images. This main objective can be reached by defining following sub-objectives:

1) To evaluate the existing model and optimize it by fine-tuning its parameters for handling images from MODIS sensor in order to estimate the incident solar irradiation over an area under clear and cloudy sky conditions.

2) To estimate appropriate parameterizations to estimate the instantaneous radiation for different regions in different time period for clear and all sky conditions.

3) To estimate daily solar radiation from the instantaneous radiation.

1.2.2. Research questions

1) What are the optimum parameterization and its required parameters to estimate the net surface shortwave radiation (NSSR) using MODIS data and products?

2) Is the model behaving as expected (experimental error obtaining by the observed responses from the predicted responses)? How is the model behaviour affected by any assumptions required for fine-tuning of the model?

3) How to validate the results considering the spatial, temporal, and spectral characteristics of the ground measurements compared to the MODIS data and its products?

4) What are the methods and how to reduce uncertainty in daily and monthly interpolation algorithm from the instantaneous radiation using, for example, the sinusoidal model?

2. LITERATURE REVIEW

2.1. Satellite remote sensing in solar radiation calculation

The amount of solar energy received by a surface at the ground level depends on the orientation of the surface to the Sun, the hour of the day, the day of the year, the latitude at the point of observation and the atmospheric conditions. In the early morning or late afternoon, the solar radiation reaching the Earth's surface follows an oblique, longer path through the atmosphere. As a result the atmospheric attenuation is greater and the intensity is significantly reduced (Iqbal, 1983). Recent developments in the areas of photochemistry, photobiology and satellite remote sensing have also helped in bringing attention to calculation or estimation of solar radiation.

Now a days this satellite data usage have higher demand for solar radiation calculation because of satellite sensors are precisely calibrated and maintained during the whole life-cycle, data delivery is stable. On the other hand this geostationary satellites provide near-real-time global coverage data, which allows monitoring, now-casting and forecasting. Hence this satellite based solar radiation estimations getting more popular than the traditional point base measurements.

A number of methods for estimating solar radiation from satellite data have been developed by Tarpley (1979), Cano. et al. (1986), Cess et al. (1991), Noia et al. (1993), Li. et al. (1993b), Zelenka et al. (1999), Rigollier et al. (2004) and Janjai (2010).
Duguay (1995), Bisht et al. (2005), Houborg et al. (2007), Wang and Liang. (2009), Keunchang. et al. (2010), Bisht and Bras (2010) and Bisht and Bras (2011) have developed methods to calculate net radiation (R_n), key component in Earth energy budget (Figure: 1) and its elements in all sky conditions. Downward shortwave radiation showed the largest error contribution in estimated net solar radiation (Bisht & Bras, 2011). This is one of the main problems in calculating net solar radiation. The near surface MODIS data products used by Wang et al. (2005), Wang and Pinker (2009) and Qin et al. (2011) to produce estimates of various components of the surface energy budget for clear days.

Several researchers have contributed to estimating net surface shortwave radiation (NSSR) from satellite observed radiance and atmospheric and surface variables (Cess et al., 1991), (Li et al., 1993a), (Rigollier et al., 2004), (Todd et al., 2009), (Tugjsuren & Batbayar, 2011). A review conducted by Pinker et al. (1995) and recently by Shunlin et al. (2010) have shown the development of those approaches.

Tang et al. (2006), Kim. (2008), Wang and Pinker (2009), Todd et al. (2009), Tugjsuren and Batbayar (2011), Tianxing et al. (2012) and Huang et al. (2012) have estimated NSSR by using MODIS data and its products. A statistical regression approach between the MODIS TOA radiance and reflectance to estimate NSSR by Tang et al. (2006) for clear and cloudy days has shown to have a lower RMSE than the Bisht and Bras (2010) methodology.

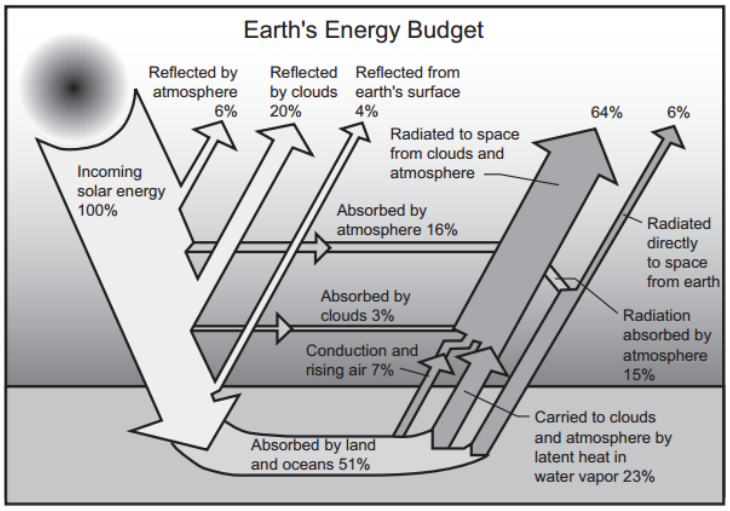

Figure 2-1: Components of the globally averaged energy budget. (Source: www.sundogpublishing.com)

To deliver calculation of accurate instantaneous net shortwave radiation, Kim and Liang (2010) has developed hybrid algorithm for both clear and cloudy sky using MODIS data but authors mentioned that uncertainty in the model causes effect of the atmospheric heterogeneity. Meanwhile Tianxing et al. (2012) developed a consistent retrieval method to estimate radiant flux under clear sky conditions.
For retrieving these solar radiation from space, numerous attempts have been made to deliver accurate instantaneous net radiation during past decades and these methods can be grouped into four categories (Tianxing et al., 2012).

(1) **Empirical methods**; Brutsaert (1975), Hamon et al. (1954) and Tarpley (1979); these models are simple to operate; the results are site-specific and cannot be apply for different regions. Some of these models are theoretical, dealing with the solution of the radiant transfer equation and linking satellite radiance and surface radiant fluxes.

(II) **Physics-based methods**; Pinker and Ewing (1985), Dedieu et al. (1987) and Duguay (1995); theoretically, these methods are accurate but depend strongly upon driving parameters and are often computationally expensive and complex.

(III) **Parameterized methods**; Sridhar and Elliott (2002) , Bisht et al. (2005), Bisht and Bras (2010) and Bisht and Bras (2011); these models are computationally efficient compared to the physics-based methods. Parameterized scheme based on atmospheric parameters.

(IV) **Hybrid methods**; Li et al. (1993a), Wang and Liang. (2009), Tang et al. (2006), and Kim and Liang (2010); generally such methods employ radiant transfer simulation followed by statistical modeling. This method does not required ancillary data. Hybrid methods showing possibility of produce accurate solar irradiation calculation for clear sky conditions.

2.2. Solar radiation calculation based on satellite remote sensing

Estimating solar radiation is based on remote sensing method is the most practical and reliable, because remote sensing observations are higher to ground based observations for acquiring the features of global scale (Liang, 2004). Since the 1960s, meteorological satellites have greatly expanded and numerous attempts at deriving surface solar irradiance using satellite data have been made using either statistical approaches by Cano. et al. (1986), Noia et al. (1993) or physical model by Gautier et al. (1980). Approaches made of higher resolution products from the Geostationary Operational Environmental Satellite (GOES) by Cano et al. (1994) and Gautier and LandSfield (1997), and the Meteorological Satellite (METEOSAT) Rigollier et al. (2004). Houborg et al. (2007), mentioned that satellite based estimation of solar radiation higher than ground based pyaranometer observations. Roerink et al. (2012) and Bojanowski (2013) validated solar radiation estimates retrieved from METEOSAT second generation data.

Multiband sensors, such as the Spinning Enhanced Visible and Infrared Imager (SEVIRI) sensor carried on the METEOSAT Second Generation satellite and MODIS sensors are also used to generate surface radiation products (Liang. et al., 2006).

To have an improved temporal scan, geostationary satellites, are fixed above a given point on the equator, they continuously scan the exposed part of the Earth surface. The resulting data stream has a high temporal frequency typically one full scan every 15–30 min enabling diurnal monitoring of cloud characteristics and movement, and the generation of time and site-specific irradiance data and a spatial resolution of 5–10 km. The geostationary satellites view the Earth's surface at an increasing angle with increasing latitude causing a gradual degradation of spatial resolution and data reliability due to positioned above the equator. In this situation, geostationary satellites for solar estimation provide less accuracies at high latitudes.

2.3. MODIS data in solar radiation calculation

The Earth Observing System (EOS) is a program of NASA including a series of satellite missions and scientific instruments in Earth orbit designed for long-term observations on the Earth. MODIS is a system of two imaging spectrometer components designed to research tasks that require long term, low resolution and global, multi-spectral data sets and the MODIS instrument is operating on both the Terra and Aqua spacecraft in sun-synchronous orbit (URL-1).

MODIS is designed to scan through nadir in a plane perpendicular to the velocity vector of the spacecraft, with the maximum scan extending up to 55° on either side of nadir (110° aperture). It has a viewing cross track and along track swath width of 2330 km and 10 km respectively and views the entire surface of the Earth every 1 to 2 days. MODIS has 36 spectral bands with centre wavelengths ranging from 0.412 μm to 14.235 μm. Two of the bands are imaged at a nominal resolution of 250 m at nadir, five bands are imaged at 500 m, and the remaining bands at 1000 m (Ahmad et al., 2002).

MODIS data and products downloaded from NASA missions of the EOS and images are typically distributed as HDF (Hierarchical Data Format) 10° x 10° tiles, projected in the sinusoidal projection.

The many data products derived from MODIS observations describe features of the land, oceans, and the atmosphere and products are available from several sources. As well as, available at different collection, or version, processing levels. Data for version 4 and above have been validated and approved for scientific research (URL-2). Major advantage is to use MODIS derived atmospheric optical properties to achieve automated and operational correction at the global level (Kaufman. & Didier., 1998), to achieve accurate NSSR or its components. Research described in this paper has selected MODIS land and atmospheric data products only.

2.4. Solar Radiation measuring Instruments (Radiometers)

This section refers to WMO (2008) published by World Meteorological Organization (WMO), produce guidance to making meteorological, climatological, hydrological and geophysical observations, as well as the exchange, processing and standardization of related data.
To measure the radiant flux (power) of electromagnetic radiation by a radiometer, absorbs solar radiation at its sensor, transforms it into heat and measures the resulting amount of heat to ascertain the level of solar radiation. The radiometers used for general measurements are pyrheliometers and pyranometers that produce direct solar radiation and global solar radiation, respectively.

2.4.1. A Pyranometer

A pyranometer is a type of actionmeter (actinometers are instruments used to measure the heating power of radiation) used to measure broadband solar irradiation on a planar surface and is a sensor that is designed to measure the solar radiation flux density (W m^{-2}) from a field of view of 180°. For analysing the amount of solar radiation available at a particular site, the pyranometer could be mounted at the same orientation as a solar panel would be mounted.
The fundamental needs are for the sensor to be level, free of vibration and free of any obstruction above the plane of the sensing element including both fixed features. Therefore, a tall, stationary and easy access platform like the top of a tall building is perfect. It may be impossible to avoid the temporary obstruction of direct beam solar radiation impinging on an up-facing radiometer by masts, antennas, flag poles and similar structures.

2.4.2. A Pyrheliometer

Direct solar radiation is best measured by pyrheliometers, the receiving surfaces of which are arranged to be normal to the solar direction. The predicted uncertainties are based on the assumptions such as (I) maintaining condition of instruments, correctly aligned and clean surface, (II) 1 minute and 1 hour figures are for clear sky irradiances at solar noon, and (III) values of daily exposure for clear sky days at mid latitudes.
There are two types of instruments: (I) Primary standard pyrheliometers, which an absolute pyrheliometer can define the scale of total irradiance without resorting to reference sources and (II) the secondary standard pyrheliometers which an absolute pyrheliometer which does not satisfied the specification for a primary standard can be used as a secondary type. Operational pyrheliometer measurements are based on following characters of the instrument such as; (I) The field of view of the instrument, (II) Measuring capability of both the long-wave and shortwave portion of the spectrum, (III) The temperature compensation or correction methods and (III) The magnitude and variation of the zero irradiance signal..

2.5. Calibration of pyrheliometers

In generally, recommends a minimum calibration cycle of five years but annual calibrations is better for highest measurement accuracy All pyrheliometers, other than absolute pyrheliometers, must be calibrated by comparison using the Sun as the source. The procedures for the calibration of field pyrheliometers are given in an ISO standard (ISO-1960:1990) and (ISO-9847:1993).

3. MODIS DATA SELECTION AND STUDY AREA

3.1. MODIS data and products in land domain

The most important interaction between the land and atmosphere involves the exchange of energy and moisture. Accurate measurements of relevant parameters is essential in order to better understand of magnitude of those interactions. MODIS Terra circles Earth in a polar orbit (from north to south) and Aqua is in a geostationary pattern (around the equator). MODIS provides several land surface characteristics, including surface reflectance, the percent of total solar energy that is reflected back from the surface, called albedo and land surface temperature etc. Significant progress has been made in estimation of those land-atmosphere related characteristics by using satellite based methods including MODIS data from space and MODIS morning(Terra)/ afternoon(Aqua) acquisition method which is designed to take advantage of the unique capability of the MODIS instrument(Wan, 1999).

3.1.1. Land surface Temperature

A long term data set of satellite derived land-surface temperature, such as that from MODIS can be used to answer critical issues about the regional-global climate changes. At the same time, this satellite measured surface temperature used to improve models and methods for evaluating land-surface energy balance (Diak & Whipple, 1993).
In order to meet the requirement for Land Surface Temperature (LST) in climate, hydrologic, ecological and biogeochemical studies in both clear-sky and cloudy conditions, a meteorological model forecasts shows capability of incorporate LST for such applications (White et al., 1993). Hence MODIS LST can be used as an input to update the metrological model over areas under clear-sky conditions and the metrological model provides forecasts of LST values for areas under cloudy atmospheric conditions. Climate models with land-surface temperature data have provided valuable information for making modifications in the optical properties of clouds in the solar and radiative transfer parameterization (Hahmann et al., 1995).
Cloud cover is a common problem for visible and infrared remote sensing and MODIS LST as well as other MODIS land products only available in clear sky conditions. Therefore, the MODIS LST in MOD11 products can be used as binary cloud-no cloud image identifier. To use the mask effectively, user have to understand and define proper tolerance for cloud or clear when performing to define image as cloudy or clear sky. MOD11_L2, at 1 km spatial resolution used in this study to determine cloudy or clear situation in image.

3.2. MODIS data and products in Atmospheric domain

Earth's net radiation budget is significantly moderated by the atmosphere's interaction with incoming and outgoing radiation. Changes in the balance of net radiation, many atmospheric characteristics such as clouds, water vapour and aerosols play significant influences.

MODIS daily global coverage combined with its high temporal resolution and carefully selected spectral bands will significantly improve understanding of clouds. Cloud measurements are also important because clouds often obscure the Earth's surface, complicating observations of land surface conditions and also the largest uncertainty in the estimation of NSSR. MODIS cloud detection capability is so sensitive that it can even detect clouds that are indistinguishable to the human eye (Rebecca & David, 2000). In addition to its observations of clouds, MODIS also measures cloud optical thickness and aerosols, which influence solar radiation both directly and indirectly.

Daily scenes of MOD021KM, MOD03, MOD05_L2 and MOD11_L2 product files provided by the NASA, Level 1 and Atmosphere Archive and Distribution System (LAADS), (URL-2) were selected for this research because they are readily available free of charge and have a good temporal and regional coverage.

The MOD021KM products, calibrated Earth view data by the MODIS Characterization and Support Team (MCST), including the 250 m and 500 m resolution bands aggregated to appear at 1 km resolution, are TOA radiances and reflectance (Toller et al., 2006). The first seven spectral bands of MOD021KM used this study to calculate TOA reflectance and described in Appendix 1(Kim., 2008).

For the geo-location fields include geodetic latitude, longitude, surface height above geoid, solar zenith and azimuth angles (cell to Sun), sensor zenith and azimuth angles (cell to sensor), for each 1 km grid from MOD03 , calculated for each 1 km MODIS Instantaneous Field of View (IFOV) for all daytime orbits (URL-2). The solar zenith and azimuth angles, satellite zenith and azimuth angles are used to estimate NSSR in this study.

The MOD05_L2 products are the near-infrared retrieval total column precipitable water product consists of vertical column water vapor amounts in cm at 1 km spatial resolution over clear land areas of the Earth, and above clouds over land (Gao & Kaufman, 1990).

This research has adopted above described MODIS data products to retrieve the shortwave broadband albedo and calculate net surface shortwave radiation by using the parameterization mentioned in Tang et al. (2006) model and generation of daily interpolated radiation data from the instantaneous and daily radiation retrieved by combination of above MODIS products.

3.2.1. Top of Atmospheric (TOA) albedo.

The planetary albedo consists two major sections due to atmospheric reflection and a due to surface reflection by using shortwave radiance at the surface and TOA. The ratio of reflected to incident shortwave radiation at the TOA, the planetary albedo is the fraction of incident light from the Sun which is reflected back into space by the Earth.

Surface reflection makes a relatively small contribution to planetary albedo because the atmosphere attenuates the surface contribution to planetary albedo by a factor of approximately three. The huge amount of the observed global average planetary albedo (88%) is due to atmospheric reflection (Aaron. & David, 2011).

The TOA broadband albedo and the precipitable water in early researches as Li et al. (1993a), (Li. et al., 1993b) and (Masuda et al., 1995) utilized from the Earth Radiation Budget Experiment (ERBE) satellite data and the European Centre for Medium Range Weather Forecast (ECMWF) data, respectively. However, the data we used in this research paper are MODIS data, which are narrowband reflectance at the top of atmosphere. To obtain TOA broadband albedo as input for model simulation, narrowband reflectance must be converted to shortwave broadband albedo.

3.3. Study site and data description

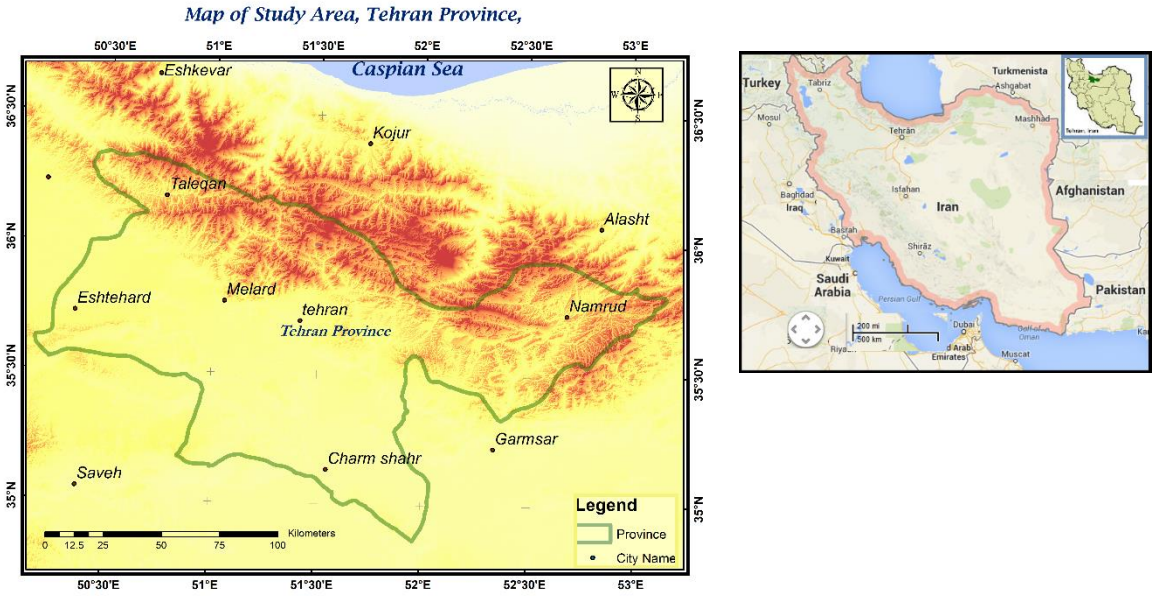

Figure 3-1: Map of Iran and Study area, Tehran Province, (Source; Http:// www.clubs.psu.edu)

Tehran Province, the study area chosen for this study is located to the north of the central plateau of Iran. Country Iran extends in latitude from about 24° to 40° N and in longitude from 44° to 64° E. (Figure: 3-1). It is one of the world's most mountainous countries. The area Tehran Province, under study lies between 35° 1' to 36° 20' N and in longitude from 50° 10' to 51° 08' E that is one of the thirty provinces and most densely populated region in Iran.

3.3.1. Climate condition

Tehran features a semi-arid, continental climate. Tehran's climate is largely defined by its geographic location, with the Alborz Mountains to its north and the central desert to the south. It can be generally described as mild in the spring and autumn, hot and dry in the summer, and cold in the winter. Summer is usually hot and dry with very little rain, (Figure: 3-2) but relative humidity is generally low and the nights are cool. Tehran's climate can be described to have some monsoon influences; the summers are very dry, and the spring and fall are rather lush, with the main precipitation occurring at this time.

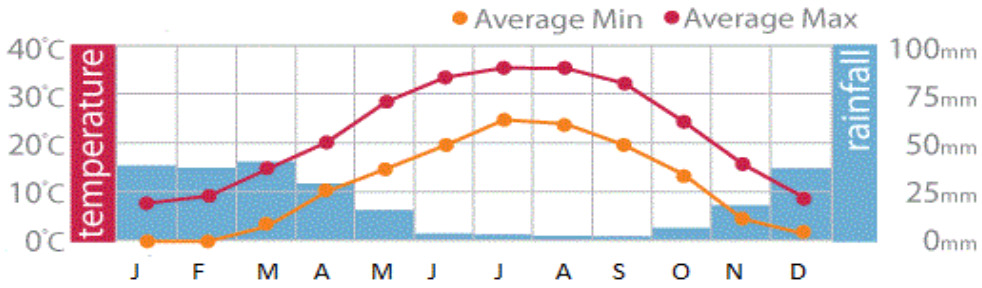

Figure 3-2: Average temperature and rainfall of Study Area. (Source; Http:// www.intrepidtravel.com)

3.4. Image selection

The MODIS datasets used for the study area consists of MOD021KM; Reflectance data, MOD03; Geo-location data and MOD 05;Total perceptible water (Water Vapor) and MOD11, during the day overpass time has downloaded from NASA web sites (URL-2) and apply for NSSR model development. MOD02, MOD03, MOD05 and MOD11 data covering 30 days on July, August and September months of year 2013 have selected.

Table 3-1: Selected MODID Image description for model implementation

Short Name	Long Name	Channel Data	Resolution
MOD021KM	MODIS/Terra Calibrated Radiances 5-Min L1B Swath 1 km	1 to 7	1 km
MOD03	MODIS/Terra Geo-location fields 5-Min L1A Swath 1 km	none	1 km
MOD05_L2	MODIS/Terra Total Perceptible Water Vapor 5-Min L2 Swath 1 km	17,18 and 19	1 km
MOD11_L2	MODIS/Terra land surface temperature and emissivity , 5-Min L2 Swath 1 km	31 and 32	1 km

3.5. Meteorologialcal data

Meteorological data for model validation obtained from ground point measurements at northern part of the Iran. The study site is over the northern part of Iran covering most of the Tehran city limit (Figure: 3-1). For validate the study, ground station named Chitgar (35.76 ° Latitude and 51.20 ° Longitude) within the Tehran Province limit was used.

The highest point of the province is Mount Damavand, at an elevation of 5678 m above mean sea level and the lowest point of the province is the plains of Varamin, 790 m above mean sea level. Average annual rainfall is approximately 200 mm and the province has a semi-arid climate. Relative humidity is generally low and the nights are cool and the hottest month is July (temperature, 26°C to 36°C) and the coldest is January (temperature, -1°C to 8°C).

Ground measured solar radiation data recorded every 10 minutes was stored in year 2013 include with air temperature, wind speed, diffuse radiation, global radiation and reflect radiation. Instantaneous net shortwave radiation is retrieved through the global radiation minus the reflected radiation. Daily average NSSR values also retrieved from monitoring of same ground measured data.

For the model validation purposes SURFRAD data downloaded from SURFRAD network. Penn State site (described in Chapter 8) in USA have chosen to download the ancillary data.

4. CONCEPT AND METHODOLOGY

4.1. Relationship between TOA and surface radiation

Solar radiation at the surface and TOA vary approximately linearly as the Solar Zenith Angle (SZA) changes (Cess & Vulis, 1989). Practical solar radiation calculations require knowledge of the solar zenith angle for any location, time of day, and day of year. MODIS data provide this information for calculations.
The TOA solar irradiation expressed as:

$$F(t) = S_0 \left(\frac{r_0}{r}\right)^2 \cos(\theta_Z) \quad (1)$$

Where, $F(t)$ TOA solar irradiance, S_0 is the solar constant, mean Earth-Sun distance r_0 , and θ_Z is the solar zenith angle. The Earth-Sun distance *r* varies throughout the year according to the elliptical orbit.
S_0 , is the amount of solar radiation received outside the Earth's atmosphere on a surface normal to the incident radiation per unit area and per unit time at the mean Earth–Sun distance. This solar irradiance depends strongly on the solar zenith angle and also on the ratio (r_0/r) of the actual distance to the mean distance of the Earth from the Sun.

4.1.1. Solar Zenith angle and the day length

From spherical trigonometry the solar zenith angle varies with the season as well as during the day. As a result, the incoming solar radiation field is very smooth. The solar zenith angle θ_Z is a function of time, day number and latitude (Figure 4-2). It can be calculated using the relation:

$$\cos(\theta_Z) = \sin\delta \ \sin\varphi + \cos\delta \cos\varphi \cos\omega \quad (2)$$

Where δ, is the solar declination of the Sun, φ the geographic latitude, defined as positive in the northern hemisphere and ω the solar hour angle. The latter is a measure of the local time, i.e. it is defined as the angle through which the Earth must turn to bring the meridian of the location of observation directly under the Sun. The solar declination (Figure: 4-1) is a function of the day of the year and is independent of the location.

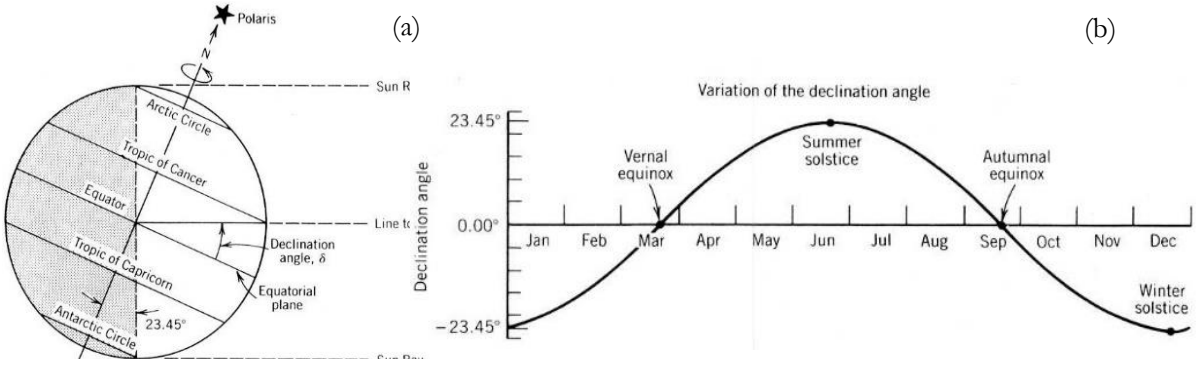

Figure 4-1: Solar declination angle (a) and variation of declination angle throughout the year (b). (Source: www.powerfromthesun.net)

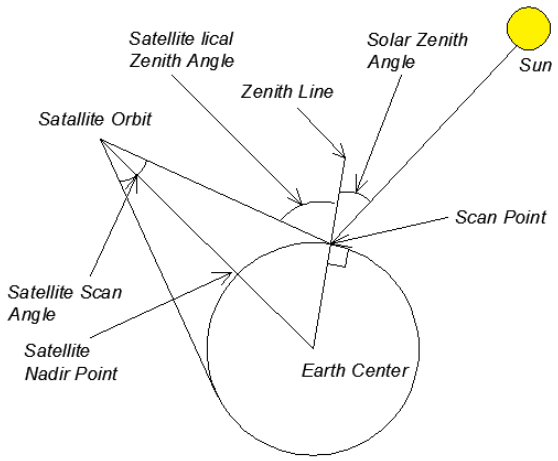

Figure 4-2: Solar Zenith Angle and other solar geometry

Where the Astronomical day length L_d is calculated by the following formula

$$L_d = \left((24/pi) * \cos^{-1}(\tan(\varphi) * \tan(\delta))\right) \quad (3)$$

Here, solar declination angle, δ in degree is define as,

$$\sin^{-1}(0.39795 * \cos(2pi * (N - 173)/365.25))$$

φ = latitude of the point in degree, *N* is the Julian day of the year and L_d, astronomical day length (hr). Day length model could be used to determine daily radiance. Solar declination angle, δ from MCB model described by William. et al. (1995) have used to estimate day length in this research. MOD03, geo-location data provide the latitude of point.

4.2. Net Surface Shortwave Radiation (NSSR) estimates

The components of the radiation balance are derived using a radiative transfer models and algorithms that estimate energy fluxes from remotely senses data, (R_n) is estimated by combination of its shortwave and long-wave components;

$$R_n = [R_S^{\downarrow} - R_S^{\uparrow}] + [R_L^{\downarrow} - R_L^{\uparrow}] \quad (4)$$

Where, R_n = Net radiation [$\mathrm{W\ m^{-2}}$].
$R_S^{\downarrow}$ and $R_S^{\uparrow}$ = Downward and upward shortwave irradiance [$\mathrm{W\ m^{-2}}$], (0.3-3.0 μm)
$R_L^{\downarrow}$ and $R_L^{\uparrow}$ = Downward and upward long-wave irradiance [$\mathrm{W\ m^{-2}}$], (3.0-50 μm)

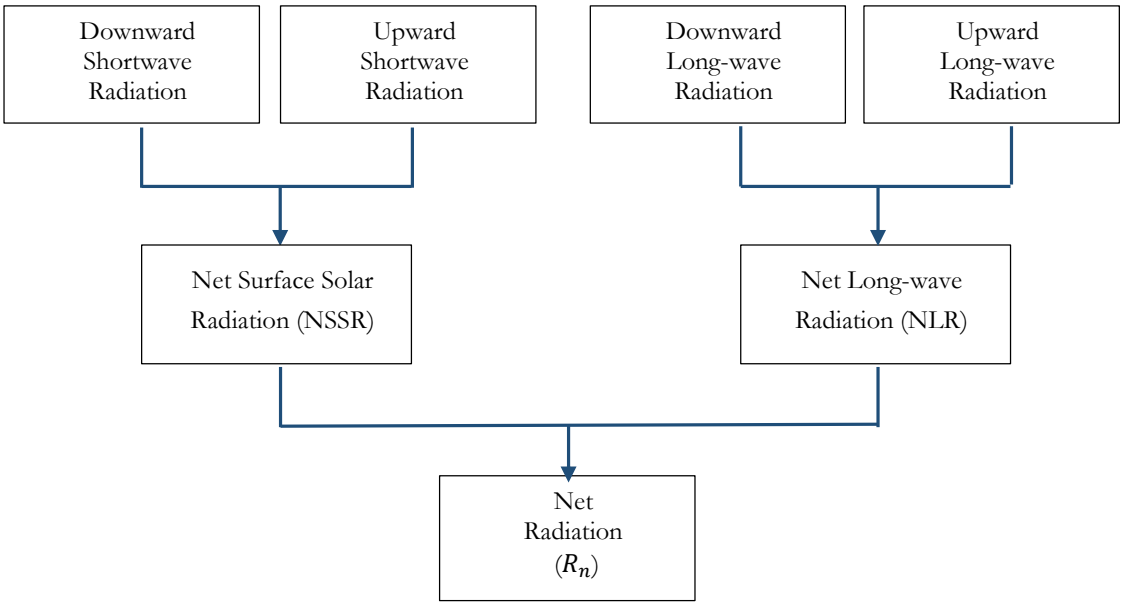

Figure 4-3: Net Radiation (R_n) and its components

Four components, mentioned in top of the Figure: 4-3, makes the contribution to the calculation of net radiation (*Rn*) at the surface. The more interesting field is that of the net surface shortwave radiation that is, the difference between the incoming shortwave solar radiation at the Earth's surface and the reflected part.

Shortwave radiation (visible light) contains a lot of energy than long-wave radiation (infrared light). It is one of the most important parameters for climate studies and it controls the total energy exchange between the atmosphere and land/ocean surface. The latter is a function of the planetary albedo which is strongly a function of the atmospheric structure and clouds. There is no downwards solar radiation in night time and the only source of outgoing solar radiation is reflection. Therefore night time net solar radiation is zero.

This thesis specially deals with net surface shortwave radiation component ($R_S^{\downarrow}$ and $R_S^{\uparrow}$) in net radiation equation (*Rn*) for clear and cloudy sky conditions. Estimates of this component is essential for both real time and short term forecasts for energy usage modeling and optimization in the solar energy industry.

4.2.1. Instantaneous NSSR

Tang's statistical algorithm (Tang et al., 2006) is the selected empirical algorithm for this research to calculate NSSR is based on the Li's parameterization (Li et al., 1993a) and (Masuda et al., 1995). This kind of hybrid models have proved effective to accurately estimate solar radiation at several locations (Kim., 2008).

According to the mentioned method, the incident irradiance absorbed part at the surface denoted as a fraction of the irradiance incident at the TOA related to the outgoing irradiance at the TOA and the local planetary albedo r', expressed as;

$$a_s(\mu, w_e, r) = \alpha' - \beta' r' \tag{5}$$

Where, (a_s) is the fraction of the incident irradiance absorbed at the surface and, α' is the intercept and β' is slope. Hence r' represent as,

$$r' = \frac{F_u d^2}{E_0 \cos\theta_s} \tag{6}$$

F_u is upwards flux at the TOA, precipitable water column, w_e and TOA broadband albedo, r' measured directly from various satellite observations.

Then the *NSSR* is defined as,

$$NSSR = \frac{a_s E_0 \cos(\theta_s)}{d^2} \tag{7}$$

Where, (θ_s) solar zenith angle, (E_0) is the TOA solar irradiance at one astronomical unit, *d* is the Earth–Sun distance in astronomical units.

The intercept (α') and slope (β') in equation (5) were stated that,

$$\alpha' = 1 - a_1\mu^{-1} - a_2\mu^{-x} - (1 - e(-\mu))\left(a_3 + a_4 w_e^y\right)\mu^{-1} \tag{8}$$

$$\beta' = (1 + a_5 + a_6 \ln\mu + a_7 w_e^z) \tag{9}$$

Where, μ is the cosine of the solar zenith angle, w_e is the column water vapor amount and $a_1 to\ a_7$ are constant for various surfaces. In the initial parameterization equation developed by Li et al. (1993a) expressed in terms of parameters x, y, and z were assumed as 0.5 but later they were treated as free parameters by Masuda et al. (1995) in that improved parameterization. In order to adopt above parameterization for this study, by calculating w_e and, r', the narrowband reflectance at TOA from MODIS data which used in this stage must be converted to shortwave broadband albedo.

4.2.2. Shortwave broadband albedo

Broadband albedo is a key forcing parameter controlling the planetary radiative energy budget and its partitioning between the surface and atmosphere. Many researches have retrieved TOA broadband albedo with several steps including scene identification, atmospheric correction and narrowband to broadband conversion. Several steps may leads to increase errors in final albedo estimates.
MODIS data in this research are narrowband reflectance at TOA have to be converted narrowband to broadband in different atmospheric and geometric conditions. TOA broadband albedo have computed by Tang et al. (2006) using MODTRAN 4 according to the equation (6), definition of the broadband albedo.
The first step in estimation of NSSR was to convert the narrowband apparent reflectance at the TOA to shortwave broadband albedo. To calculate TOA broadband albedo *r'* as a linear relationship expression, obtained by,

$$r' = b_0 + b_1\rho_1 + b_2\rho_2 + b_3\rho_3 + b_4\rho_4 + b_5\rho_5 + b_6\rho_6 + b_7\rho_7 \quad (10)$$

In this non nonparametric regression, where ρ_i is the TOA narrowband reflectance of MODIS band *i* and *r'*denotes the TOA broadband albedo and b_i is the corresponding conversion coefficient. Coefficient values of b_0 to b_7 have applied for pairs of Viewing Zenith Angle (VZA) and Solar Zenith Angle (SZA) in forward directions. An exponential function was used to established relationships between obtained coefficients and VZA.

$$b_i = (C_{1i} + C_{2i}) / (1 + \exp\left(\left({}^{1}/_{\cos VZA} - C_{3i}\right)/C_{4i}\right)) \quad (11)$$

Where, VZA is obtained by following formula,

$$\sin VZA = \left(\frac{R_0 + h}{R_0}\right)\sin(\beta)$$

R_0 is a Earth radius, h is an orbital height of the satellite above the Earth and β is a sensor zenith angle.

For this research, constants c_{1i} - c_{4i} (i = 0 to 7) for given solar zenith angle 0°, 10°,20°,30°,40°,50°,60° and 70° obtained from the look up table (LUT)(Appendix-2) provided by Tang et al. (2006) and considered that the converted narrowband to broadband in different atmospheric conditions from reflectance at TOA have higher accuracy. Huang et al. (2012), have used model coefficients developed by Tang et al. (2006) with same constants in different seasons such as Eastern China monsoon region and Western China arid region and provide high accurate results (average Root Mean Square Error (RMSE) value yield by 81.2 W m^{-2}) for calculated NSSR from MODIS data in clear and cloudy skies.

4.3. Daily average net radiation (DANR) estimates

Daily average net radiation (DANR) is a fundamental driving variable for simulation of carbon ratio, water, and heat fluxes at local as well as regional, and global scales. Compared with instantaneous net surface shortwave radiation (INSSR), DANR has more practical applications for atmospheric and water cycle modeling, water resources management, quantifying land surface evapotranspiration (ET) and specially solar energy usage from satellite data and products.
The method for estimating DANR from INSSR values at 1 km resolution is presented in this study.

4.3.1. Sinusoidal model for estimating the diurnal cycle of NSSR

DANR can be applicable to estimate evapotranspiration values (ET) from MODIS data by Bisht et al. (2005) used a diurnal surface temperature estimation scheme that was first developed by Lagouarde and Brunet (1993) in order to estimate a diurnal cycle of *Rn*. In this thesis, sinusoidal model have choose to estimate the diurnal cycle of NSSR for clear and cloudy sky days considering maximum NSSR value during the day as;

$$NSSR(t) = NSSR_{\max} \sin\left[\left(\frac{t - t_{rise}}{t_{set} - t_{rise}}\right)\pi\right] \tag{12}$$

Foe particular day, t_{rise} is the local time of sunrise which make NSSR positive and t_{set} is the local time of sunset which make the NSSR value negative and during the day, $NSSR_{\max}$ denoted is maximum value of NSSR (Figure: 4-4). To perform DANR, from instantaneous NSSR, the value of $NSSR_{\max}$ should be calculated.
Terra local equatorial crossing time is approximately 10:30 a.m. in a descending node with a sun-synchronous, near-polar, circular orbit. Therefore satellite overpass time are available as model input. Before build the relationship between instantaneous NSSR and DANR; maximum NSSR given as:

$$NSSR_{\max} = \frac{INSSR}{\sin\left[\left(\frac{toverpass - t_{rise}}{t_{set} - t_{rise}}\right)\pi\right]} \tag{13}$$

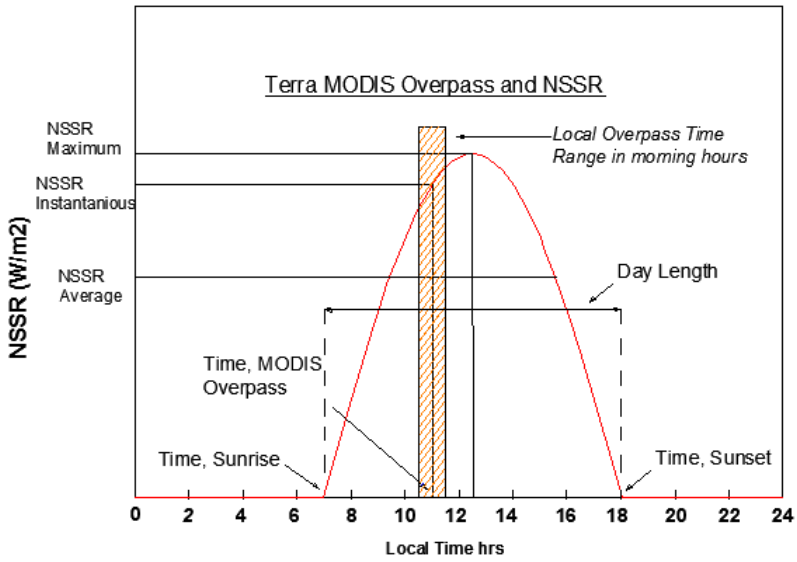

Figure 4-4: Sinusoidal model with MODIS overpass and Day length

Daily average net radiation given as:

$$DANR = \frac{\int_{t_{rise}}^{t_{set}} NSSR\,(t)\,dt}{\int_{t_{rise}}^{t_{set}} dt} = \frac{2NSSR_{\max}}{\pi} = \frac{2INSSR}{\pi \sin\left[\left(\frac{t_{overpass} - t_{rise}}{t_{set} - t_{rise}}\right)\pi\right]} \quad (14)$$

Consider day length (d_L), the difference between t_{set} and t_{rise} and the difference in time between when NSSR is the maximum value and MODIS overpass local time as *A*. Then the equations (14) can be rewritten as,

$$DANR = \frac{2INSSR}{\pi Sin\left[\left(\frac{DL - 2A}{2DL}\right)\pi\right]} \quad (15)$$

According to the climate condition (seasons), the day and night are not exactly of equal length at the time of the March and September equinoxes. The relationship between season, day length and solar radiation is straight forward. When days get closer to winter, days get shorter and having less hours of daylight reduces the amount of solar energy throughout the day. As an example, Table 4-1 provide year round hours of daylight at 35° N for every 15 day period.

Table 4-1: Day light variation throughout the year in 35° N Latitude.

Latitude 35° N						
Date	**1-Jan**	**16-Jan**	**1-Feb**	**16-Feb**	**1-Mar**	**16-Mar**
Hours light	09.69	09.89	10.27	10.73	11.18	11.74
Date	**1-Apr**	**16-Apr**	**1-May**	**16-May**	**1-Jun**	**16-Jun**
Hours light	12.34	12.89	13.40	13.84	14.18	14.34
Date	**1-Jul**	**16-Jul**	**1-Aug**	**16-Aug**	**1-Sep**	**16-Sep**
Hours light	14.33	14.14	13.77	13.32	12.77	12.21
Date	**1-Oct**	**16-Oct**	**1-Nov**	**16-Nov**	**1-Dec**	**16-Dec**
Hours light	11.65	11.1	10.56	10.13	09.82	09.66

Source: http://www.orchidculture.com/

The INSSR and DANR depend on the day length d_L and *A*, Eq. (15). The day length varied from 14 hours in summer and 9 hours in winter. It has observed that the maximum NSSR generally occurred at 12:30 p.m. local time., The ground observation data was aggregated over 10 minutes time interval and MODIS overpass for Iran ranged from 10:20 to 11.30 local time for the study region, The study period of 30 days (mentioned in Chapter 6) sweep over three months.

4.4. Sensitivity analysis.

Sensitivity Analysis (SA) focus is on analysis of sensitivity of the variations in the system parameters of scalar model outputs (Saltelli et al., 2000). Main goal of such kind of analysis is to identify among input parameters the most sensitive to model outputs, those for which a little variation may involve a great change in model result. In this research, method of sensitive analysis is utilized here under technique of Morris method. The Morris method by Morris (1991) for sensitivity analysis is a so called one-step-at-a-time (OAT) method, meaning that in each run of model, only one input parameter is given a new value.

The method performed by sampling a set of start parameter values within the defined ranges of possible values for all input variables and calculating the subsequent model result.

Then in the nest stage, changes the values for one parameter and all other inputs parameters remaining at their start values and calculates the resulting change in model result. Next, the values for another parameter are changed and at the same time the previous parameter kept at their start value. This steps can apply all the parameters in the model.

The OAT method deals efficiently with environmental models containing many of input parameters without relying on strict assumptions about the model and this method is simple to understand and implement, and its results are easily interpreted. Furthermore, it is economical in the models have number of few parameters but more time consuming in models have more parameters. On the other hand one parameter at a time does not allow for identification of correlation between parameters are the limitations of this approach.

In this research, sensitivity analysis of existing model was performed to assess the impact of errors or variation of the model. In each model run, ±10% around the base input value of existing parameter value was considered. New model coefficients has introduced after SA approach and mentioned in Chapter 7.

5. DATA PREPARATION

5.1. Downloading MODIS images

Daily scenes of MOD021KM, MOD03, MOD05_L2 and MOD11_L2 product files downloaded from NASA, LAADS web site (URL-2). Most of the MODIS data are gridded data, which they have been processed into a latitude-longitude grid.

MODIS filenames (i.e., the local granule ID) follow a naming convention which gives useful information regarding the specific product. For example, the filename of MODLAND level 2 products;

MOD07L2.A2006001.0735.005.2006012234657.hdf indicates:

MOD07L2 -	Product Short Name and processing level
.A2006001 -	Julian Date of Acquisition (A-YYYYDDD)
.0735 -	MODIS acquisition UTC time
.005 -	Collection Version
.2006012234567 -	Julian Date of Production (YYYYDDDHHMMSS)
.hdf -	Data Format (HDF-EOS)

5.1.1. Image georeferencing and noise removal

Each MOD02, MOD03 ,MOD05 and MOD11 images open in ENVI environment and Geo-referencing using inbuilt facility to georeference MODIS. It was found that the detectors in Terra MODIS band 5 (1.230~1.250 μm) are noisy, due to sensor failure, there are sharp and repetitive stripes over the entire image (Figure 5-1). As the MOD05_L2 product has derived from these band the strips line are available in reading for Total column precepitable water vapor-near infrared retrieval layer (water vapor band) too. Therefore to reduce this noises, Low Pass Filter was applied.

.

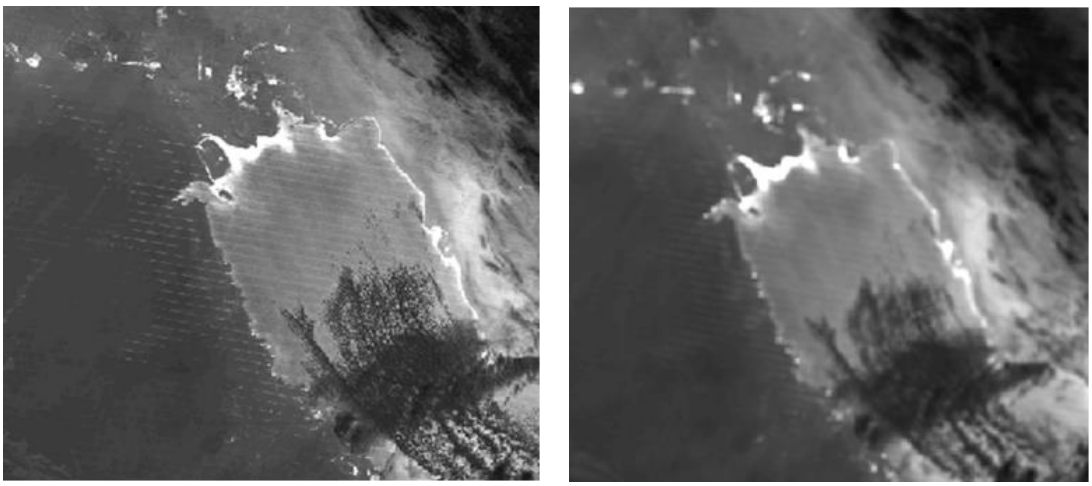

(a) (b)

Figure 5-1: MOD05 image noise, (a) original noisy image, and (b) after apply 3*3 Low pass filter.

5.1.2. Extracting the relevant bands and layer stacking

As inputs for the Tang model, 12 bands from MOD02, MOD03 and MOD05 products have selected. Reflectance bands 1 to 7 (level 1B calibrated radiance) selected from MOD021KM and there spectral range and spatial resolutions are presented in Table 5-1.

Table 5-1: MODIS bands 1 -7, Spectral Ranges.

Band #	1	2	3	4	5	6	7
Spectral Range (nm)	620-670	841-876	459-479	545-565	1230-1250	1628-1652	2105-2155
Ground Resolution(m)	250	250	500	500	500	500	500

The MODIS near-infrared total precipitable water product consists of column water vapour amounts from MOD05_L2. Study consist of 0.94 and 0.86 μm channel ratio for total precipitable water amount. The MODIS level 1-A product that contains geodetic information (geo-location data) such as latitude, longitude, satellite zenith and solar zenith angles from MOD03 products for all daytime orbits. Extracted relevant bands in ENVI environment and used layer stacking to build a new multiband image file from georeferenced images. Nearest neighbour resampling method was used and output file have a geographic extent that covers only the data extent where all the files overlap within the study region. Layer Stacked image has converted into Tagged Image File Format (TIFF) and exported to Mathlab environment to proceed retrieval of NSSR and DANR.

Solar radiation maps have prepared in ARC GIS environment and maps are categorised according to the Clear and Cloudy sky conditions for the Instantaneous NSSR as well as daily averaged NSSR.

6. IMPLEMENTATION OF THE ALGORITHM

This chapter mainly considers project implementation in study area, to fulfil the aims and objectives of the research. In the middle of the sections have described the detail of study period and specific MODIS data and products follow up to calculation of NSSR and DANR by improved model.

6.1. Project formulate

To achieve the objective of this research, two interrelated steps have been considered in this chapter. Firstly, remote sensing including satellite data from MODIS was used to derive instantaneous net radiation, secondly prepared NSSR and DANR maps of the study area. Figure 6-1 have represented the flowchart of methodology, implemented throughout the project.

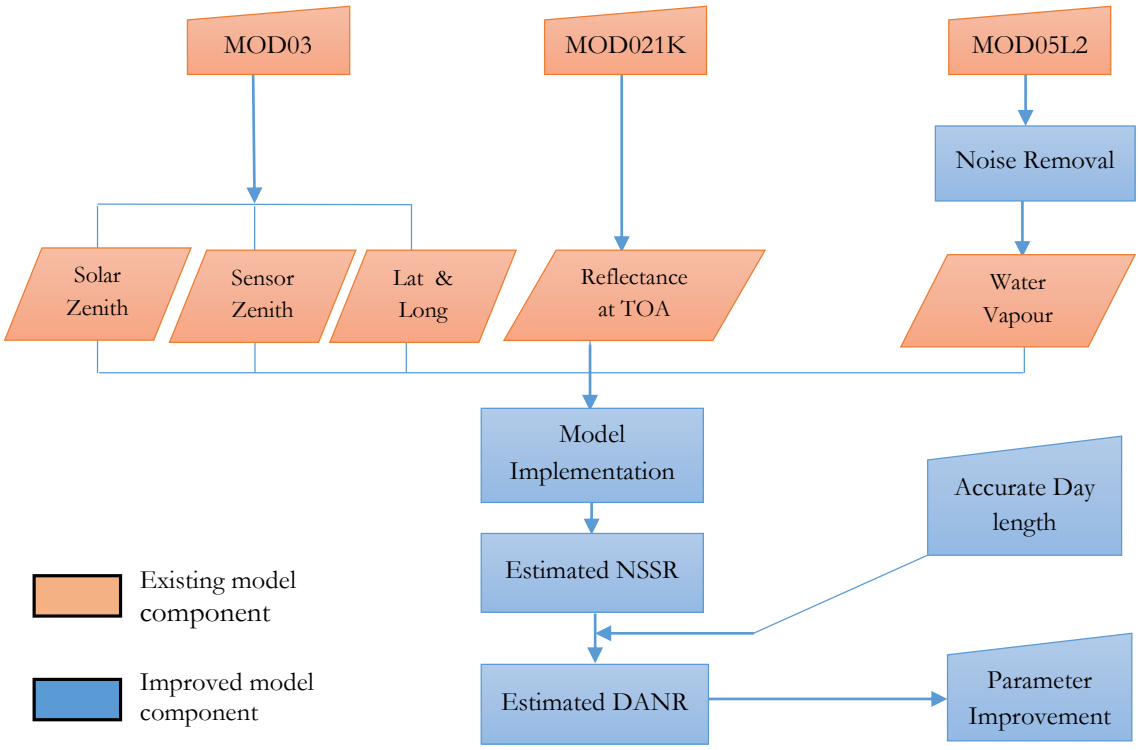

Figure 6-1: Flowchart to improved Tang's statistical algorithm for estimate instantaneous and daily average net surface shortwave radiation from MODIS data.

To achieve the first step, the MODIS images have separated cloudy and clear sky condition and then estimate the NSSR according to the all skies, cloudy sky and clear sky conditions. Error analysis and model verification have implemented for evaluation of model performance and quantitatively tested with other similar methods applied by previous researches. Error propagation analysis methods and scatter plots have provided the theoretical background and used to convince the evaluations. Produced solar radiation maps.in GIS environment for visual representations. When preparing the maps, temporal variation and spatial distribution of magnitude of solar radiation over the study region has considered.

After satisfactory analysis of model performances in NSSR estimation, DANR estimation was performed as second step. Model validation for DANR, ground based observation data have used in same period observed by one metrological station within the study region. It has observed that daily average NSSR estimates from observed data as well as INSSR estimated data are more meaningful aggregate than instantaneous NSSR estimates. At the same time it has been noted that that sunset and sunrise time related to the local sunrise and sunset times and are approximated as 1 h after local break of the day time and 1 h before the time in the evening at which the Sun begins to fall below the horizon, respectively. This 1 h time period slightly vary according to the day length also but it has not render more influence on the average NSSR estimates.
Therefore, 10 minutes interval observed data per particular day have rearranged as 'positive part' without considering the observed data before sunrise and after sunset. This average value was used to model validation on estimated DANR from MODIS data in Iran. DANR maps have prepared according to specifications of NSSR maps for selected days (described in Chapter 7), for cloudy and clear skies.

The methodology was applied to 16 clear sky days and 14 cloudy sky days for MODIS day overpass in the year 2013, which ranges from July to September. Total number of acceptable cloudy and clear overpasses are 15, 17 and 08 images on July, August and September months respectively The criteria for determining a clear sky was that at least 75% of the study area should be free from cloud pixel described as Bisht et al. (2005) and MOD11 LST data used to determine this tolerance. The MOD11_L2 data product is available for only clear sky pixels, hence binary measured the number of pixels in MOD11 image for which land surface temperature was available. This binary marked values used to build threshold indicator to separate image as cloud or non-cloud over the study region (Figure: 6-2).

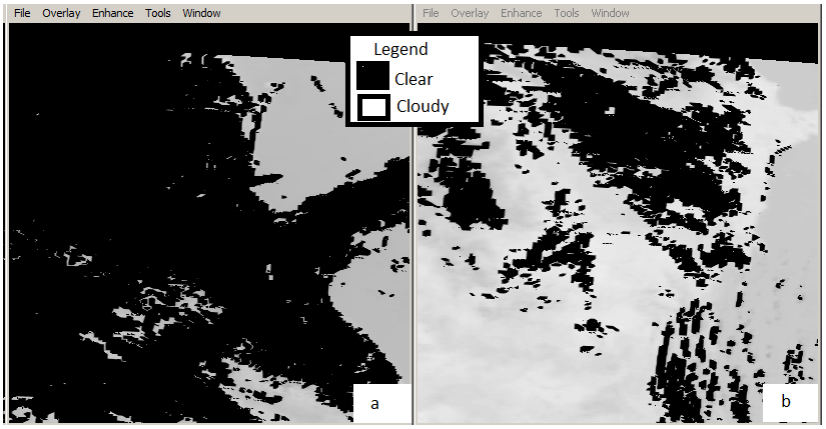

Figure 6-2: MOD11, LST measurement and sky condition on study region. (a) Clear sky-calendar day, 198 and (b) Cloudy sky-calendar day 239.

Detail description of study period and MODIS acquisition UTC time over the study region obtained from the MODIS image description described in Table 6-1 and it contains the image sky condition, local time of sunrise (T_{rise}) and sunset (T_{set}) for the each day. Sunrise (T_{rise}) and sunset (T_{set}) and observed day length for the each day obtained from the website (URL-3), which have used for comparison of estimated day length and this estimated day length has used to estimate DANR.

Table 6-1: MODIS Terra overpasses UTC time over study region for selected MODIS images and number of images per month with their sky condition. (Amount of images, 15, 17 and 08 on month of July, August and September respectively)

No	Calendar day	Month	Julian day	Sky condition	UTC time	T_{rise}	T_{set}	Observed Day length
1	**1**	July	182	Cloudy	7.05	05.52	20.24	14.5353
2	**2**		183	Clear	7.50	05.52	20.24	14.5264
3	**3**		184	Cloudy	6.55	05.53	20.24	14.5169
4	**4**		185	Cloudy	7.35	05.53	20.24	14.5064
5	**6**		186	Clear	7.25	05.54	20.23	14.4833
6	**7**		188	Clear	8.05	05.55	20.23	14.4706
7	**10**		191	Clear	7.00	05.57	20.22	14.4278
8	**13**		194	Clear	7.40	05.59	20.21	14.3786
9	**17**		198	Cloudy	7.05	06.01	20.19	14.3039
10	**18**		199	Clear	7.50	06.02	20.19	14.2833
11	**19**		200	Cloudy	6.50	06.03	20.18	14.2625
12	**22**		203	Clear	7.25	06.05	20.16	14.1958
13	**23**		204	Clear	8.05	06.05	20.16	14.1725
14	**26**		207	Clear	7.00	06.08	20.14	14.0994
15	**29**		210	Clear	7.30	06.10	20.11	14.0217
16	**2**	August	214	Clear	7.05	06:13	20:08	13.9114
17	**7**		219	Clear	7.25	06:17	20:03	13.7644
18	**14**		226	Cloudy	7.30	06:22	19:55	13.5444
19	**18**		230	Cloudy	7.05	06:25	19:50	13.4122
20	**20**		232	Clear	6.55	06:27	19:48	13.3450
21	**23**		235	Clear	7.25	06:29	19:44	13.2422
22	**27**		239	Cloudy	7.00	06:32	19:39	13.1028
23	**3**	September	246	Cloudy	7.05	06.38	19.29	12.8525
24	**5**		248	Cloudy	6.55	06.39	19.26	12.7800
25	**8**		251	Cloudy	7.25	06.42	19.22	12.6706
26	**12**		255	Clear	7.00	06.45	19.16	12.5233
27	**19**		262	Cloudy	7.05	06.50	19.06	12.2639
28	**21**		264	Cloudy	6.55	06.51	19.03	12.1897
29	**24**		267	Clear	7.25	05.54	17.58	12.0778
30	**28**		271	Cloudy	7.00	05.57	17.53	11.9289

Model validation and analysis of model performances for NSSR estimation, the SURFRAD network data have used. The SURFRAD network has been named the primary validation network to support satellite retrieval validation, modeling, and climate, hydrology, and weather research over the United States for the Clouds and the Earth's Radiant Energy System (CERES) instrument aboard the NASA Earth Observing System (EOS) satellites TRMM (Tropical Rainfall Mapping Mission), Terra, and Aqua (John et al., 2000). The quality of SURFRAD data has been recognized through its acceptance by large and reputable scientific organizations and many universities for their research purposes. The primary observations are the incoming and outgoing components of broadband solar and thermal infrared irradiance. Hence, for model validation purposes in this thesis SURFRAD data was used.

7. RESULTS AND DISCUSSIONS

This chapter describe the analysis conducted the results calculated for the algorithm and compared with the ground observations. Estimated NSSR is described in the Section 7.1 and estimated DANR is described in the Section 7.2. Comparison of NSSR and DANR, observed and the MODIS derived with (a) at satellite overpassing time in the study region (b) daily estimated by analysing their Bias, correlation coefficient (R^2) and RMSE of observation are also presented. Furthermore, this chapter gradually addresses the issues of main objective of this thesis, and the maps of NSSR and DANR for the study region is also presented. Developed model parameters using sensitivity analysis process mentioned in latter part.

7.1. Instantaneous net surface shortwave radiation (NSSR) estimation

Shortwave radiation is the sum of a direct beam component and a diffuse component. Both components depend on surface-atmospheric energy exchange. Net Surface Shortwave Radiation is required to estimate the energy exchange between the atmosphere and land surfaces. An accurate estimate of NSSR at high spatial resolution is essential in regional and global environmental models.
The intention of the current research and study attempt to estimate the instantaneous net surface shortwave radiation (INSSR) and daily average net radiation (DANR) using Terra MODIS data. In order to address this issues, instantaneous MODIS TOA spectral radiance was converted to TOA total shortwave albedo with the help of coefficients of the TOA narrow-to-broadband conversions for different solar zenith angles in forward direction provided by the Tang et al (2006). Then the instantaneous net surface shortwave radiation was computed using the parameterization mentioned in equation (6) in Section 4.2.1. To obtain the coefficients x, y, z and a_1 to a_7 for equation (8) and (9) as discussed in Chapter 4, and those parameter values are mentioned in Table 7-1.

Table 7-1: Coefficients for estimating the NSSR from the TOA broadband albedo (Tang et al., 2006).

Surface	a_1	a_2	a_3	a_4	a_5	a_6	a_7	x	y	z
Land	−0.011	0.179	−0.980	0.929	−0.701	0.090	0.846	0.478	0.052	−0.020

The aim of this research as mentioned in research objectives is, to obtain NSSR maps for over large areas. As described in Chapter 4, an effort is being made to understand and mitigate differences between calculated and observed radiance. Instantaneous NSSR maps have prepared after having successful model output. An example of the INSSR map for the study region on 17 th July, 2013, is shown in Figure: 7-2 and retrieved values from MODIS image to calculate NSSR for this day in particular pixel on Chitgar metrological station referred in Table 7-2. The dark region in the north side of the map, refers to the Caspian Sea.

Table 7-2: Calculated model output for meteorologialcal station at Chitgar on 07 th July, 2013

Description	Station
Latitude	35.7640°
Longitude	51.2052°
Day Length	14.1637
SZA/VZA	25° / 43°
TOA albedo	0.2201
Water vapour	0.2212 (g/cm^2)
NSSR	723 (w/m^2)
DANR	603.4 (w/m^2)

Performances of the improved model estimates quantitatively tested with the available ground observations. The ground measurements for the evaluation of the estimated values have obtained from the metrological station established in Chitgar (35.76 N, 51.20 E) in province of Tehran and every 10 minutes recorded ground measurements have used for the comparison of NSSR and DANR values retrieved from model. Final results were evaluated according to their Bias, Root Mean Square Error (RMSE), and linear correlation coefficient (R^2).

Table 7-3 presented the overview of statics between estimated and observed NSSR for (a) both sky, (b) clear sky and (c) cloudy sky conditions. Same results as shown in Figure: 7-1, scatter plots showing the Bias, R2 and RMSE for each situation.

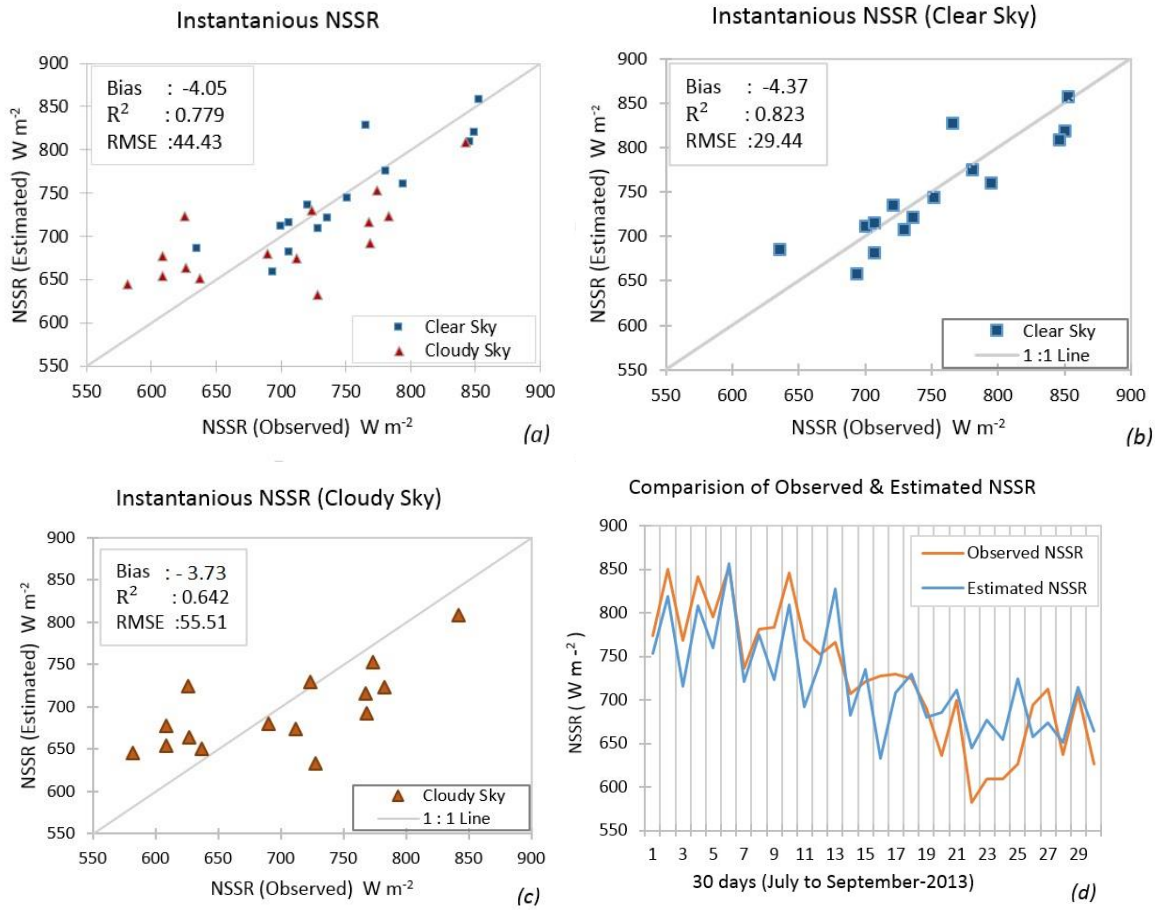

Figure 7-1: Scatterplot with regression. Instantanious NSSR estimated for (a) both skys, (b) clear sky (c) cloudy sky and (d) comparission of NSSR for 30 days period mentioned in Table 6-1.

Figure 7-1 shows the scatter plots of the results for NSSR estimated for 30 days period in Tehran province area throughout the three months of period from July to September, 2013. According to the detailed results are listed in Table 7-3, in clear-sky conditions, the average RMSE value yielded by 29.44 W m^{-2} and average RMSE value yielded by 55.51 W m^{-2} in the cloudy sky condition. In the clear sky, model estimated NSSR performed better than the cloudy sky condition and it's nearly double the accuracy of estimation of NSSR. But in the clear sky model average Bias value (- 4.37) slightly higher than the average Bias value (- 3.37) in cloudy condition as Figure 7-1 (b) & (c). But less variation in the clear sky estimation than the variation in the cloudy sky condition.

Additionally, in variation of estimated results in cloudy condition, correlation coefficient, R^2 shows lower value than clear sky condition. Although the linear correlation is higher in clear sky condition than cloudy condition. This stronger association indicating a more linear relationship between the observed and measured NSSR. At the same time it shows that the correlation is positive means the value of observed increases, the estimated value also increases in the same direction. In this thesis the correlation coefficient is an abstract measure and it is not given to a direct precise interpretation because without large number of estimations, furthermore, more observations increases the correct evaluation.

Table 7-3: Quantitative comparison of estimated NSSR with ground observation in the study area.

Station	**Clear & Cloudy sky**			**Clear Sky**			**Cloudy Sky**		
	Bias (W m^{-2})	R^2	RMSE (W m^{-2})	Bias (W m^{-2})	R^2	RMSE (W m^{-2})	Bias (W m^{-2})	R^2	RMSE (W m^{-2})
Chitagr	- 4.05	0.779	44.43	- 4.37	0.823	29.44	- 3.73	0.642	55.51

In initial model applied by Tang et al. (2006) mentioned that RMSE less than 20 W m^{-2} and 35 W m^{-2} for clear sky and cloudy sky respectively. Same model tested in Eastern China by Huang et al. (2012), the corresponding values are 81.2 W m^{-2} and 113.2 W m^{-2} for clear sky and cloudy sky respectively.

Hence, RMSE values for this thesis estimated for NSSR, lies between this two previous studies. Those two previous studies and this research have used same model coefficients to estimate NSSR as described in Chapter 4. Carefully analyzing the Figure: 7-1(a) and (b), it has shown slightly underestimated results, at the same time, similar overestimated results have described by Huang et al. (2012) in his analysis using same model but different locations in different seasons and mentioned that the need of identifying and evaluation of seasonal changes as well as atmospheric conditions for reliable estimated model outputs. Figure: 7-1(d) represented that overall estimated NSSR throughout the 3 months period. In the month of July it shows underestimated model results but end of the September it was overestimated behavior. This is a good representation of different model behavior in different seasons. In the beginning of the study period the day length increases and the model results shows underestimation behavior, but in the latter part of the study period, the day length decrease and the model shows overestimated behavior.

For any particular region, a bias value about ±9% is still considered as a good model performances. It may increase to ±15% or more based on any adverse conditions, on an annual basis (Cebecauer et al., 2011).

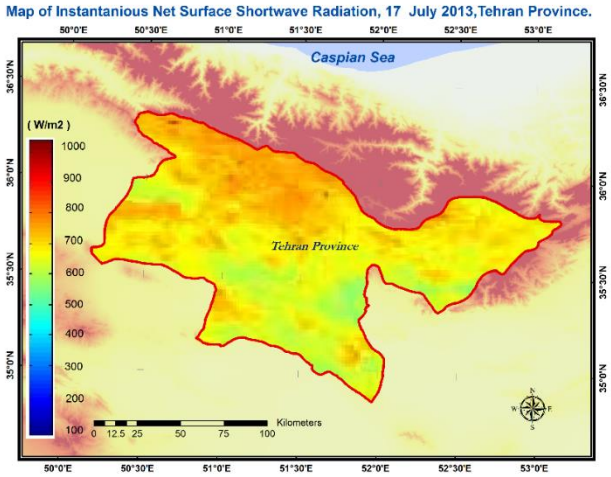

Figure 7-2: Map of Instantaneous Net Surface Shortwave Radiation, 17 th July, 2013, Tehran Province.

For visual interpretation of estimated NSSR, solar radiation maps were prepared. The NSSR maps demonstrated reasonable tendency in deviation of estimated NSSR values depend on the geographical features also. The significant factors that contributed to the value of NSSR can be analyze using the NSSR maps up to some reasonable level. The highest estimated NSSR values were found in the areas near the Caspian Sea as well as in higher elevations (Figure: 7-2).

7.2. Diurnal cycle and Daily Average Net Radiation (DANR) model

The value of NSSR received changes greatly through the day and year due to weather patterns and the changing position of the Sun. Net long-wave radiation is fairly constant and negative. During the daylight hours, NSSR providing positive values and this magnitude depend on the latitude of the observation location, day of the year, sky condition as cloudy or clear and time of day. Hence depend on the seasonal changes this resulting diurnal pattern of NSSR shows strong variations. At every turn of the seasons, the length of the daylight period and sunrise and sunset times that day has is different (William. et al., 1995).

7.2.1. Relevance of Sinusoidal model and day length

It has proven that sinusoidal model applicable to estimate the diurnal cycle of NSSR , hence, the suggested sinusoidal model in this research, similar to physical based method initially proposed by Lagouarde and Brunet (1993) and developed by Bisht et al. (2005) as described in Chapter 4 has used to estimate diurnal cycle of NSSR, for both clear and cloudy sky days. In the sinusoidal model, the NSSR values before t_{rise} and after t_{set}, in local time were assumed to be close to null.

The calculation of accurate day length, the approximate time between t_{rise} and t_{set} is one of the key input to calculate DANR and value of day length calculated from equation (3) described in Chapter 4.
This day length depend on the Latitude and solar declination angle of particular location. Day length and Sun elevation for any given location and day can be known in advance.

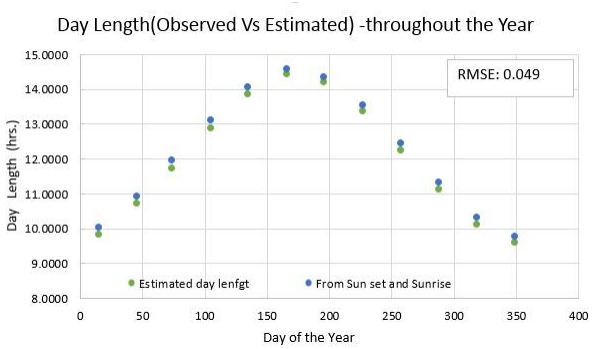

Figure 7-3: Monthly day length variation throughout the year, difference of estimated and observed by the model.

Estimated day length (L_d) for one day for each month for the study area (15 day of each month) has calculated to test the model suitability and Figure: 7-3 represent the variation of day length throughout the year and RMSE 0.049. Table 7-4 described the error differences and maximum difference is 0.2209 hours (12 minutes).

Table 7-4: Day length comparision with estimated length obtained by this reserch and observed fron sunrise and sunset time for the whole year.

Month	Day of Year	Day length in Hours		
		Estimated	Observed from Sun set and Sunrise	Difference
January	15	9.8284	10.0075	0.1791
February	46	10.6976	10.9036	0.2060
March	74	11.7108	11.9317	0.2209
April	105	12.8673	13.0864	0.2191
May	135	13.8504	14.0453	0.1949
June	166	14.4063	14.5628	0.1565
July	**196**	**14.2030**	**14.3469**	**0.1439**
August	**227**	**13.3572**	**13.5197**	**0.1625**
September	**258**	**12.2376**	**12.4214**	**0.1838**
October	288	11.1191	11.3117	0.1926
November	319	10.1120	10.2956	0.1836
December	349	9.5914	9.7600	0.1686

As already pointed out in the Table 7-4, the length of each day varies upon the day of the year. Day length also depends upon the definition one uses for the beginning and end of the day (Sunset and Sunrise time).

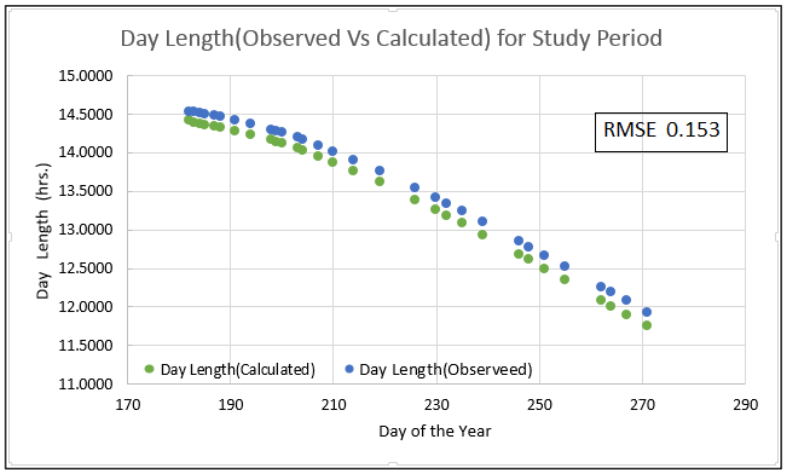

Figure 7-4: Day length variation throughout the project period over 30 days, difference of estimated and observed.

Estimated day length for the 30 days throughout the study period as shown in Figure: 7-4 and RMSE value 0.153 hours (9 minutes). Similar decreasing rate of day length as described in Figure: 7-3 has noted in the study period, so this accurate day length has used to estimate DANR values.

7.2.2. Daily Average Net Radiation estimation

In this research, DANR was calculated from single instantaneous NSSR retrieval when NSSR $_{max}$ and the DANR can be derived from the sine curve using the calculated instantaneous NSSR (clear or cloudy) at the overpass time $t_{overpass}$ in the study region.

Table 7-5 presented the overview of statics between estimated and observed NSSR for clear sky, cloudy sky as well as both sky conditions. Same results as shown in Figure: 7-5, scatter plots showing the Bias, R2 and RMSE for each situation.
According to the available results in clear sky condition and cloudy sky condition, RMSE values have shown 29.53 W m^{-2} and 31.83 W m^{-2} respectively for 30 days throughout the three months period from July to September, 2013.

Table 7-5: Quantitative comparison of estimated DANR with ground observation in the study area.

Station	**Clear & Cloudy sky**			**Clear Sky**			**Cloudy Sky**		
Chitgr	Bias (W m^{-2}) 16.2	R^2 0.770	RMSE (W m^{-2}) 30.70	Bias (W m^{-2}) 22.4	R^2 0.386	RMSE (W m^{-2}) 29.53	Bias (W m^{-2}) 10.0	R^2 0.778	RMSE (W m^{-2}) 31,83

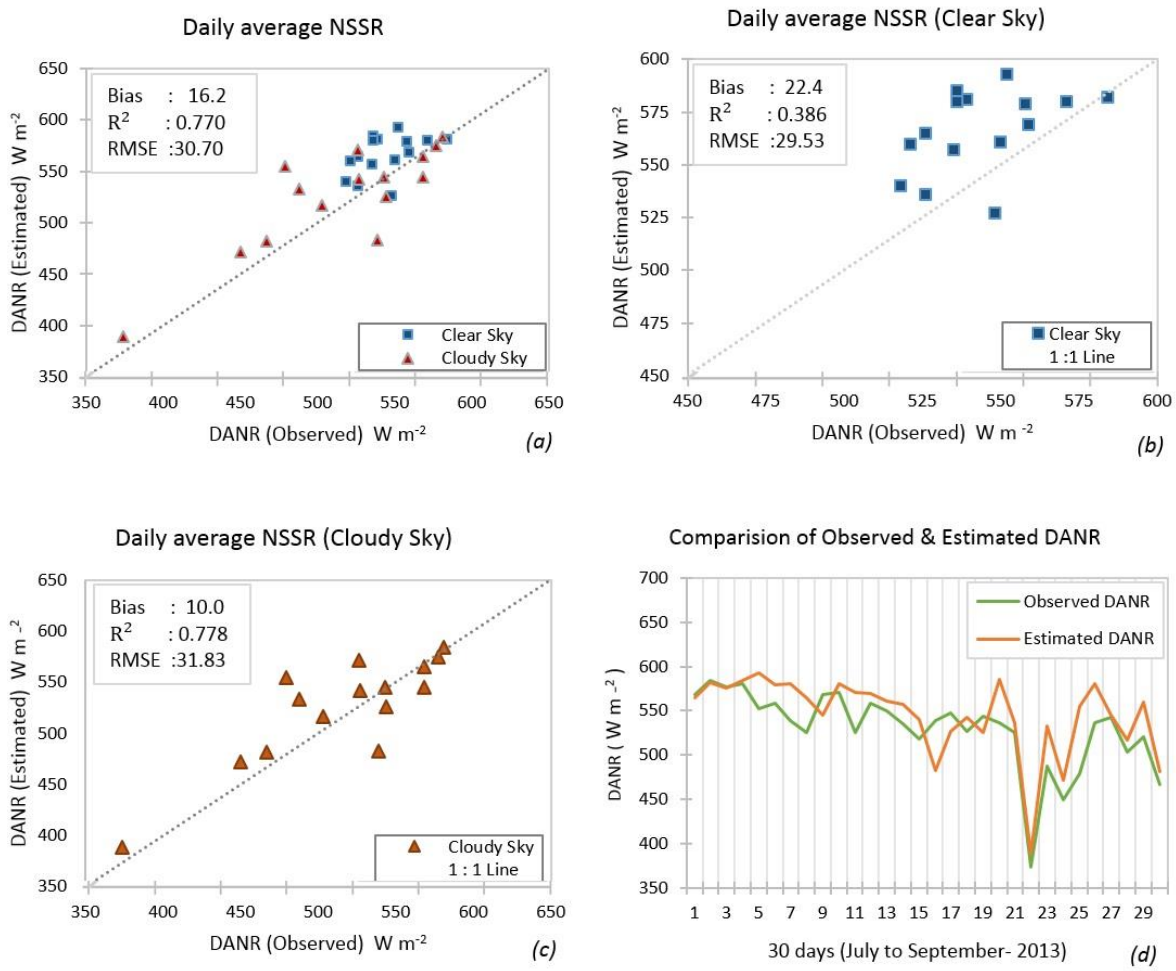

Figure 7-5: Scatterplot with regression. DANR estimated compaired with the ground observations for (a) both skys, (b) Clear sky (c) cloudy sky and (d) comparission of DANR for 30 days period mentioned in Table 7-5..

There are no publications as yet for the estimation of DANR using Tang et al. (2006) model. Therefore unable to do the quantitatively comparison of obtained RMSE values with similar results. Carefully analyzing the Figure: 7-5, it has noticed that slightly overestimated results in this estimated DANR values.
The comparison between the observed and modelled NSSR and DANR estimates for the entire study period is shown in Table 7-6. The RMSE shows that the daily average estimates of NSSR have less overall errors compared with overall errors from instantaneous NSSR in this developed method.

Table 7-6: Comparison of obtained RMSE values for estimated NSSR with estimated DANR in study period.

Station	**Clear and Cloudy Sky**	**Clear Sky**	**Cloudy Sky**
Chitgr	RMSE (W m-2)	RMSE (W m-2)	RMSE (W m-2)
NSSR	44.43	29.44	55.51
DANR	30.70	29.53	31.83

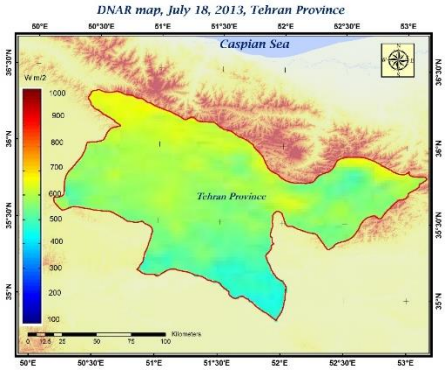

Figure 7-6: Map of Daily Average Shortwave Radiation, 18 th July, 2013, Tehran Province.

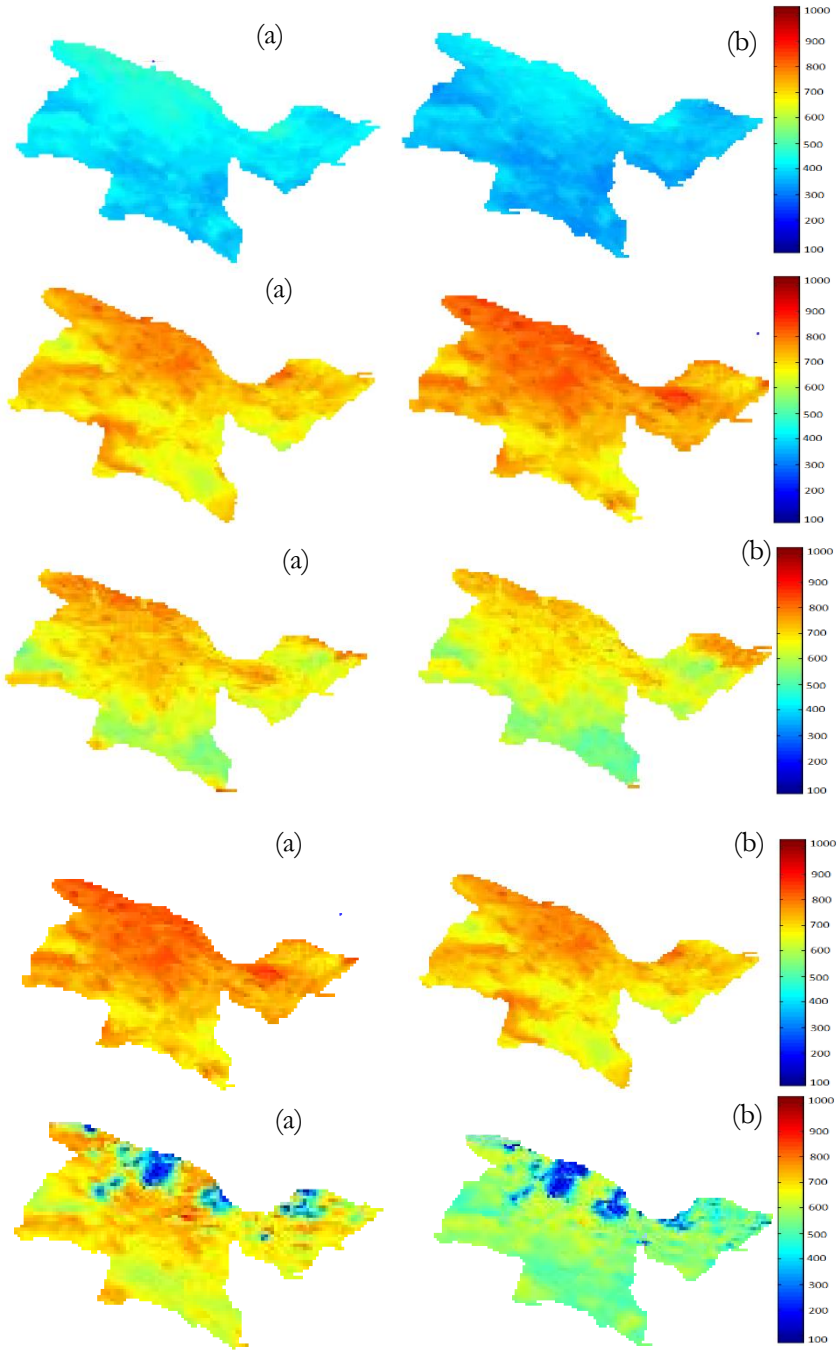

3 July , day 184,
Cloudy Sky
(a) NSSR
(b) DANR

10 July , day 191,
Clear Sky
(a) NSSR
(b) DANR

18 August, day 230,
Cloudy Sky
(a) NSSR
(b) DANR

20 August, day 232,
Cleear Sky
(a) NSSR
(b) DANR

21 September, day 264,
Cloudy Sky
(a) NSSR
(b) DANR

Figure 7-7: Spatial distribution of NSSR and Daily average NSSR according to the Sky conditions in study area.

7.3. Sensitivity analysis

Methods described as Chapter 7, NSSR has estimated for both clear and cloudy skies, slightly underestimated results have shown according to Figure: 7-1. Similar kind of overestimated results have reported by Huang et al. (2012) based on Tang et al. (2006) model. According to Table 7-3, average bias for clear and cloudy conditions are nearly - 4.37 and - 3.73 and it has decided to reduce this bias. Therefore Senility Analysis (SA) on model parameters was carried out.
Given parameters are x, y and z in the initial model by Li et al. (1993a) and described in equation (8) and (9). Parameter x have influence on solar zenith angle and parameters y and z have influences on column water vapour amount This parameter values were initially considered as 0.500 and later it was considered as free parameters by Masuda et al. (1995).

Tang et al. (2006), have proven this parameter values have 0.478, 0.052 and -0.020 for x, y and z respectively for different surfaces. Parameter x have similar value, 0.478 as in initial parameterization (0.500) but proposed different values for parameter y and z. So we assumed this different because of the different locations and different seasonal conditions.
Many of the MODIS bands are sensitive only to the column amount but not particularly to the distribution of water vapour. Above cloud precipitable water column estimates from MOD05 may be sufficient for this kind of bands (Michale et al., 1997). Precipitabal water column amount may have more influence than other parameter in this kind of models. Furthermore that the effect of cloud layer on the shortwave bands, clouds increase shortwave absorption in the atmosphere, especially in mid-latitudes, (Kato et al., 2007) and this research project lies on same region.
Therefore in this research it was decided to analysis this influence of parameter y and z and to reduce the average bias and remove the model underestimated behaviour and fine-tune the parameters according to climate condition in Iran.
Bias is a form of systematic error that can affect distort the measurement process. It is difficult or even impossible to completely remove or eliminate bias. In the process of attempting to do so, new bias may be introduced. Therefore, the goal was to minimize bias and reduced the underestimated behaviour in the developed model as well as introduced new values for parameter y and z.
It has noted that increasing the estimated NSSR amount by nearly 4 W m^{-2}, the average bias close to the zero. For this purpose sensitivity analysis have carried out on parameter y and z to choose the best values instead of 0.052 and -0.020.
The applied method (OAT) have described in section 4.4 and Figure: 7-7 and 7-8 have described the steps of procedure was applied to choose the best parameter estimation.
Model simulation on the day of 13 th July, 2013 (day of year 194) have chosen to apply OTA method and our expected NSSR value of 779 W m^{-2} from the model with new parameters and rate of parameter changes was 10% of its initial value. This new parameter values changed the estimated NSSR and aim was produce the most appropriate values with less changes on existing initial parameter values.
To assess the impact of errors or variation ±10% around base input parameter value, a sensitivity analysis was performed based on OAT method by computing NSSR value by the 9 steps for each parameter y and z. The effect on modified parameter value on estimated NSSR was analysed (Figure: 7-7 and 7-8) based on error prorogation analysis.
This simple analysis procedure offered reasonable values and aim was to reduce the magnitude of parameter variation as well as reduced the number of steps to achieve the expected NSSR value.

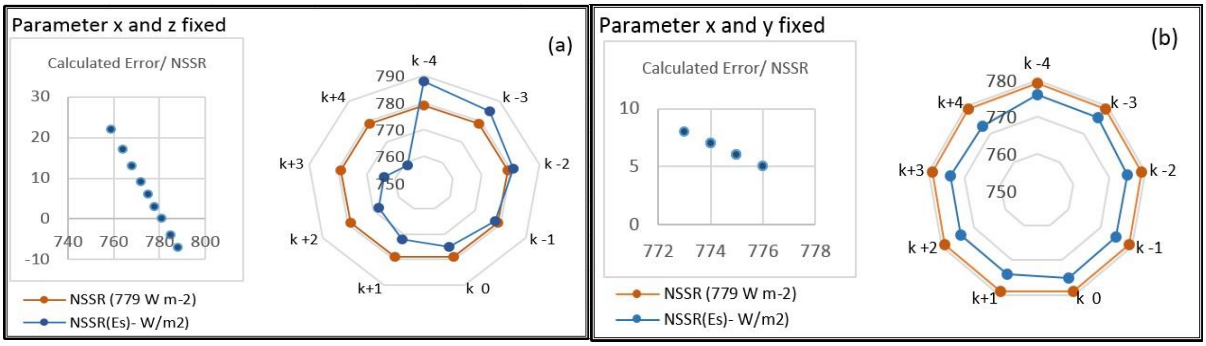

Figure 7-9: Error propagation analysis, OAT method application (a) parameter y has change, x and z remain same, (b) parameter z has change, x and y remain same.

The relative variation rate with estimated NSSR for change of only parameter x and y have shown in Figure: 7-9(a) & (b). The obtained results for parameter y changed and others are remains have shown that obtained error distribution was not linearly propagated Figure: 7-9(a) and the other case, parameter z has changed the error are not equally distributed as well as need higher value for the parameters to obtained expected value of NSSR (Table: 7-8(b)). So change of parameter y and z separately have not proven the model behaviour as expected. So next steps was identified as change both parameters together, because this both parameters have influence on water vapour content. In both cases error distribution and rate of change of the parameters have shown in Table 7-9.

Table 7-7: OAT analysis, error in estimated NSSR (a) error for parameter y has change and (b) error for parameter z has change. Parameter x and y remain same in both (a) and (b).

Step	Par-x	Par-y	Par-z	NSSR (W m-2)	Error (W m-2)
k -4	**0.478**	0.0312	-0.02	788	-7
k -3	**0.478**	0.0364	-0.02	785	-4
k -2	**0.478**	0.0416	-0.02	781	0
k -1	**0.478**	0.0468	-0.02	778	3
k -0	**0.478**	**0.052**	**-0.02**	**775**	**6**
k+1	**0.478**	0.0572	-0.02	772	9
k+2	**0.478**	0.0624	-0.02	768	13
k+3	**0.478**	0.0676	-0.02	764	17
k+4	**0.478**	0.0728	-0.02	759	22

(a)

Step	Par-x	Par-y	Par-z	NSSR (W m-2)	Error (W m-2)
k -4	**0.478**	0.052	-0.028	776	5
k -3	**0.478**	0.052	-0.026	776	5
k -2	**0.478**	0.052	-0.024	775	6
k -1	**0.478**	0.052	-0.022	775	6
k -0	**0.478**	**0.052**	**-0.02**	**775**	**6**
k+1	**0.478**	0.052	-0.018	774	7
k+2	**0.478**	0.052	-0.016	774	7
k+3	**0.478**	0.052	-0.014	774	7
k+4	**0.478**	0.052	-0.012	773	8

(b)

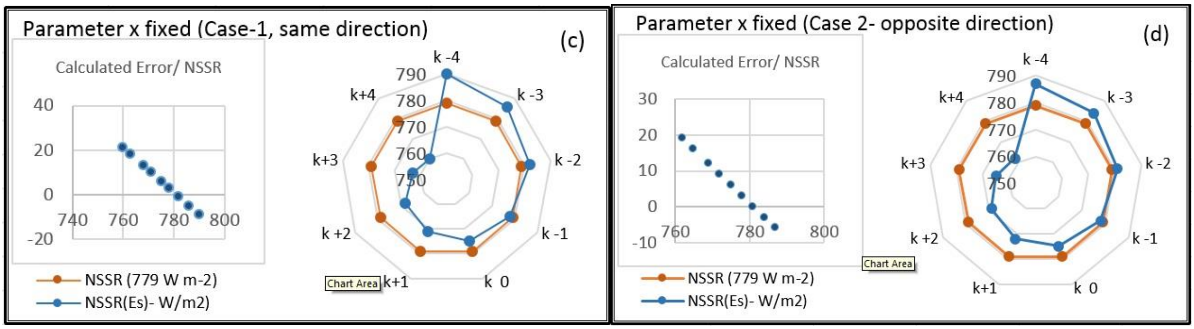

Figure 7-10: Error propagation analysis, OAT method application (c) parameter x and y has changed, both parameters change together with the same rate of increasing and parameter x remain same, (d) Both parameters change together but rate of change, one parameter value is increasing while other parameter value is decreasing and parameter x remain same.

Error propagation analysis for change of both parameters together, Figure 7-10(b) &(c) indicated error output and there variation and two stages have considered. Case (1) both parameters changed in same direction (both values increased or decreased) and, case (2) both parameters have changed in opposite direction (one increases while other decreases).

Table 7-8: OAT analysis, error in estimated NSSR, (c) both parameters changed in one direction, (d) both parameters changed opposite directions and parameter y remain same in both (c) and (d).

Step	Par-x	Par-y	Par-z	NSSR (W m-2)	Error (W m-2)
k -4	**0.478**	0.0312	-0.028	790	-9
k -3	**0.478**	0.0364	-0.026	786	-5
k -2	**0.478**	0.0416	-0.024	782	-1
k -1	**0.478**	0.0468	-0.022	778	3
k -0	**0.478**	**0.052**	**-0.02**	**775**	**6**
k+1	**0.478**	0.0572	-0.018	771	10
k+2	**0.478**	0.0624	-0.016	768	13
k+3	**0.478**	0.0676	-0.014	763	18
k+4	**0.478**	0.0728	-0.012	760	21

(c)

Step	Par-x	Par-y	Par-z	NSSR (W m-2)	Error (W m-2)
k -4	**0.478**	0.0312	-0.012	787	-6
k -3	**0.478**	0.0364	-0.014	784	-3
k -2	**0.478**	0.0416	-0.016	781	0
k -1	**0.478**	0.0468	-0.018	778	3
k -0	**0.478**	**0.052**	**-0.02**	**775**	**6**
k+1	**0.478**	0.0572	-0.022	772	9
k+2	**0.478**	0.0624	-0.024	769	12
k+3	**0.478**	0.0676	-0.026	765	16
k+4	**0.478**	0.0728	-0.028	762	19

(d)

Carefully analysis of the variation of errors, in case 1 in Figure 7-10(a) and Table:7-9(c), noted that less linearly propagated as well as obtained error differences within 9 steps larger than in the case 2 (Table: 7-10(a)). In case (2) rate of error variation of a given parameters causes the same rate of error variation and estimated error values have changed linearly for the given parameter x and y. Therefore parameter changes in opposite direction have shown the model behaviour proper way and introduced and proposed model parameters for the developed model as in Table: 7-10. Model performances for calculation of NSSR with new parameter has not discussed at this moment in this thesis.

Table 7-9: Proposed model parameters for the developed model on land surface.

Surface	a_1	a_2	a_3	a_4	a_5	a_6	a_7	x	y	z
Land	−0.011	0.179	−0.980	0.929	−0.701	0.090	0.846	0.478	0.045	−0.017

7.4. Uncertinaty analysis

Model uncertainties may affect the estimated values of solar radiation data. The amount of uncertainty may vary on the different models on same input data, but different assumptions. The only way of obtaining global and continuous information about the solar radiation or its component is by, measurements from the space using remotely sensing methods. Many transformation processes are occurred to have such a products with quantifying errors, some are related with atmospheric changes that is difficult to minimize. The uncertainties associated with such kind of quantities may lead to the errors in NSSR calculation.
In this research it has been noted those different seasons in different location has provided different error magnitudes.

Therefore, in this research, following steps have identified as key steps to leads the uncertainties of estimated NSSR as well as estimated DANR, in the process of transformation from satellite measurements to the surface solar radiation calculation by MODIS images through the developed model.

a) In initial parameterization by Li et al. (1993a), model parameters '*x*' related with solar zenith angle '*y*' & '*z*' related with water vapour content. Those values were assumed as 0.5 but later Masuda et al. (1995) treated as free parameters. Using various surface conditions, Tang et al. (2006) defined those parameters, '*x*', '*y*' & '*z*' as 0.478, 0.052 and -0.020 respectively for land surface. Theoretical study shows that different magnitudes of parameter '*y*' & '*z*' relationship is moderately sensitive to atmospheric water vapour and as well as thickness of the clouds. So various surface type with sky conditions leads the uncertainties on estimated NSSR.

b) Model inputs from MODIS data, consist with pixel problems due to the sensor failure may increase the error propagation. In this research, MOD02 products, band 05 consist with band stripping errors (image noise).

c) Another ambiguous situation was occurred; by defining of tolerance for cloudy or non-cloudy condition using MOD11, surface temperature products. This would leads to increase the model performances evaluation, but not directly to the model output.

d) Only possible way of such kind of environmental model validation is that available ground observation data. It has noted that the differences between the calculated and measured NSSR are not only the problem of these algorithms, but also there are possible opposite values between the observed and satellite estimated on spatial and temporal scales (e.g: very clear sky day, large different between observed and estimated values on day 08, September, 2013).

e) In addition, the data used by initial approach is a broadband satellite sensor data. In order to adopt this parameterization in this research, the MODIS narrowband TOA reflectance converted into the broadband TOA albedo. The errors caused by this conversion may increase the model uncertainties.

7.5. Answers to the reserch questions

Aim of this research was to fulfil the preparation of NSSR as well as DANR maps with answering following research questions. So this section mentioned, methods and procedures already have followed to achieve the said target and steps to be taken to improve the quality of main objectives of the research.

a) What are the optimum parameterization and its required parameters to estimate the net surface shortwave radiation (NSSR) using MODIS data and products?

Model used in this research to estimate NSSR using MODIS data is based on the parameterization initially developed by Li et al. (1993a) and Tang et al. (2006); only solar zenith angle and perceptible water vapour content has been considered, and assume other parameters like aerosol and gases have less sensitivity to estimated solar radiation. Therefore as described in Section 7.3(b), parameters of water vapour content have higher influence to estimated NSSR. To reduce the model underestimation, error propagation analysis can improve the amount of parameter '*y*' & '*z*'. To compute an improvement to the current best guess of optimal parameters values, the simplest approach proposed to error propagation analysis the one-at-a-time method where sensitivity measures are determined by varying each parameter independently by systematic way while all others are held constant.
Varying the input parameter by a standard amount is an easy test to perform, but this sensitivity techniques, however, become rather time consuming for large numbers of parameters. The one-at-a-time (OAT) techniques are valid only for small variability in parameter (as discussed in Section 7.3(b)) values, so this OAT method is better and the model results could be compared with the available ground data.

b) Is the model behaving as expected (experimental error obtaining by the observed responses from the predicted responses)? How is the model behaviour affected by any assumptions required for fine-tuning of the model?

As described in Figure: 7-1 in Chapter 7, model behaviour as underestimated of estimated NSSR, and previously it was overestimated in different regions in different seasons. Hence model parameters should be fine tune according to the region as well as the season of application.

c) How to validate the results considering the spatial, temporal, and spectral characteristics of the ground measurements compared to the MODIS data and its products?

Validation of satellite based estimated continuous data are difficult to be compared with point based observed data. It may leads to higher amount of surface assumptions errors and requirement of more ground based equipments in larger scale is essential as well as temporal resolution is also important. The fundamental difference between a satellite estimated and a ground measurement is that the signal received by a satellite sensor describes the average radiance over a grid cell with a significant area (e.g: 1 km x 1 km), whereas a ground station records a point based measurement.
In this research every 1 min (SURFRAD data in USA) and 10 min (in this study area) recorded ground observed data has used for model validation. Higher temporal resolution data increase the calculation of instantaneous NSSR estimations. To validate the results considering the spatial and temporal characteristics of the ground measurements compared to the MODIS data following steps have employed and results was successful.

Model validation with SURFRAD network data, it has noted that averaged observed data produced better results than single measurement in temporal scale interpolation.
Another issue was, apart from the temporal scale interpolation is the spatial scale interpolation for the comparison of the ground measured data with the MODIS sensor measurements. In this case we introduced 3* 3 average filter and run over the image on relevant pixel location and have averaged estimated NSSR and then compared the results with the SURFRAD network data. MODIS spectral characteristics such as clouds detection capability (cloud type, height, thickness) will increases the model performances as described in Section 7.3(c) that would be indistinguishable to the human eye.
Reflectance measurements from MODIS sensors contain information not only about the spectral characteristics of the surface but of the intervening TOA as well. Because these sensors are primarily used as an instrument to derive spectral reflectance information for the Earth's surface, it is advantageous to be able to detect, remove, or compensate for, the effects of the intervening atmosphere. This kind of spectral characteristic leads to increase the satellite based solar radiation estimation than ground based observations.
Furthermore, the existence of only one ground station data in the study region may leads to increase of errors of model validation process and additional ground data with a good spatial distributions are needed to cross check the model performances.

d) What are the methods and how to reduce uncertainty in daily interpolation algorithm from the instantaneous radiation using, for example, the sinusoidal model?

To reduce the uncertainty of daily interpolation it should be better first to identify what can increase the model uncertainty. In this study, analysed the various factors affecting the accuracy and uncertainty of satellite based solar radiation data. Hence following points have been considered to reduce the model uncertainties on end products of estimated solar radiation
One step is to do trend analysis of instantaneous data recorded at ground stations those are used for model validation. There are several factors considered; like long term period of observation in same pyronameter, quality control of the observations and the system of periodically maintenance of the instruments etc. Therefore, before the model validation to reduce the model uncertainty, we have been considered that evaluate the quality report of the data observed at Chitgar meteorological station.
In the other hand, in environmental modelling, interpolation introduces spatially varying errors which propagate through the model. Combination of data from different sources and different quality level may increases the model uncertainty. Therefore, in this research, application of only MODIS data and products for NSSR estimation without ancillary data reduces the model uncertainty.
Introduce suitable uncertainty analysis method to a spatial domain for quantifying spatial patterns of input variable and their behaviours within the model can control the uncertainty of the model output. If there are more ground observation data, cross validation and cross correlation method is one of the suitable methods can be applied to reduce the model uncertainty. Delete the data point at one location and estimated that point and compared. But in this research engaged with one meteorological station data and could not performed the cross validation.
Furthermore, to control the model uncertainty, MODIS images those are not well spread over the metrological station have removed from processing because, MODIS images consist with 'bowtie' effects, due to increases of view zenith angle.

8. MODEL VALIDATION

To validate the environmental models, there are no generally accepted methodologies to compare spatially distributed data with point based ground observations. Ground observation data are generally discrete and limited in number and also the measurement error associated with such measurements. Quantitative testing for such kind of model validation is acceptable and the most important component of quantitative testing is the use of observational data for comparison with model output (Bennett et al., 2013).
This research has consider model evaluation for different seasons in different regions to evaluate its higher performances. Therefore estimated NSSR was compared with measurements from one of SURFRAD sites located in Penn State (PSU) in USA (Figure: 8-1).

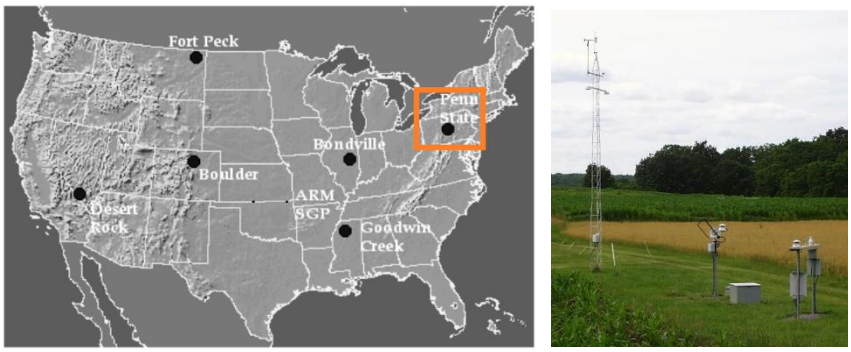

Figure 8-1: Penn State site in SURFRAD network, USA, (Source: http:/www.esrl.noaa.gov)

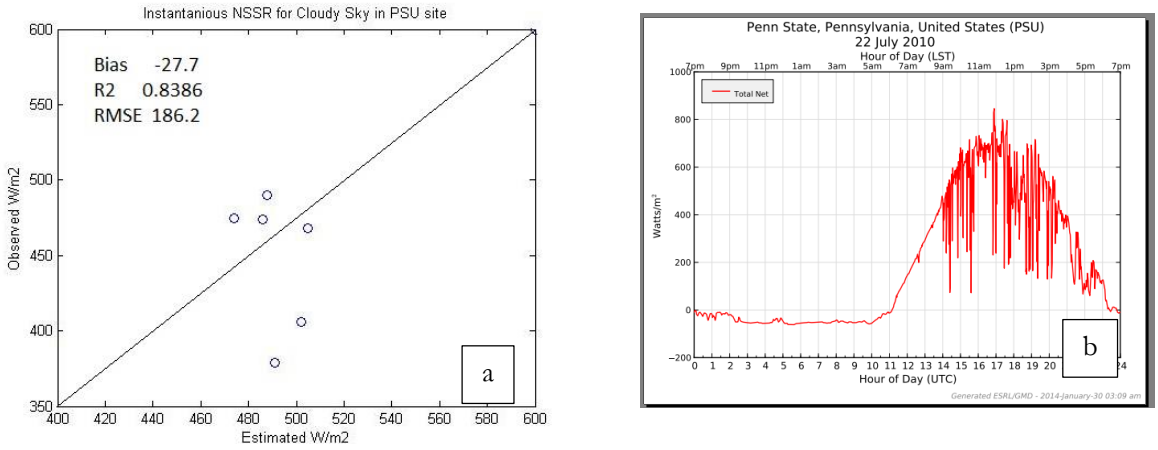

Figure 8-2: (a) Scatterplot with regression. Instantaneous NSSR with SURFRAD data and (b) Daily radiation plot of SURFRAD data, PSU site in USA.

This SURFRAD sites have a one-minute temporal resolution and SURFRAD data files contain one day of data for one station. At the same time SURFRAD provide daily Instantaneous solar radiation charts for further information (Figure: 8-2, b). Daily SURFRAD data files for this station downloaded from the location (URL-4). The comparison between the observed and the modelled NSSR is shown in Table 8-1. The Bias, Root Mean Square Error (RMSE) and correlation coefficient (R^2) for NSSR has considered.

Table 8-1: Geographic discription of SURFRAD network station PSU, USA for modal validation.

Code	Name	Latitude	Longitude	Elevation	Time zone	Installed
PSU	Penn. State University, Pennsylvania	40.72°N	77.93° W	376 m	5 hours from UTC	June 1998

Kim. (2008) have performed a similar study to test Tang et al. (2006) model using SURFRAD data in Penn State (PSU) and reported that RMSE and bias are larger than direct estimated over seven SURFRAD sites for both clear and cloudy condition. Reported R^2, Bias, and RMSE for NSSR as 0.7391, 57.9 W $m^{-2,}$ and 129.7 W m^{-2} and, while our results have a R^2, Bias, and RMSE of 0.8386, -27.7 W $m^{-2,}$ and 186.2 W m^{-2} respectively (Table 8-1) for cloudy condition only. It should be noted that Kim. (2008) performed the study for seven ground stations and mentioned that conversion from TOA radiation to broadband radiation might have atmospheric and surface lost.

Table 8-2: NSSR validation using SURFRAD data in PSU site, USA.

Paper and (Sky Condition)	Location	Period	R^2	Bias	RMSE
This paper (Cloudy)	Penn State, USA	July, 2010	0.8386	-27.7	186.2

Similar analysis by Huang et al. (2012), evaluate the Tang et al. (2006) model in Tibetan Plateau region in China and reported R^2, Bias, and RMSE for NSSR as 0.693, 50.7 W m^{-2}, and 106.6 W m^{-2} for clear sky condition and have a R^2, Bias, and RMSE of 0.557, -83.3 W m^{-2}, and 170.6 W m^{-2} for cloudy condition (Table 8-3).

Table 8-3: Tang et al (2006) method validation by previous authors.

Paper and (Sky Condition)	Location	Period	R^2	Bias	RMSE
Kim. (2008), (Clear and Cloudy)	Penn State, USA	January to June, 2005	0.7391	57.9	129.7
Huang et al. (2012), (Clear)	Tibetan Plateau region, China	January, April, July and Oct.,2004,2007,2008	0.6930	50.7	106.6
Huang et al. (2012), (Cloudy)			0.5570	83.3	170.6

9. CONCLUTIONS AND RECOMENDATIONS

9.1. Conclutions

In this research, developed method has described as practical part for estimating the daily averaged shortwave net radiation (DANR) with estimated net surface shortwave radiation (NSSR). Initially proposed method for solar radiation estimation by Li et al. (1993a) and developed by (Tang et al. (2006)) has considered in this research for NSSR estimation. Furthermore, developed hybrid model to achieve estimation of DANR from estimated instantaneous NSSR is the novelty of this research.
To retrieve daily average net surface solar radiation, improved and extend the model by combination with accurate day length calculation. Therefore to have overall advancement in this thesis, conclusion are summarized in this section.

This research main goal was early identified as estimating daily average shortwave net radiation using MODIS data and to generate solar radiation map. This study describes a method of estimating daily average shortwave net solar radiation. Accurate day length calculation improved the estimation of DANR in sinusoidal interpolation, used to produce the solar radiation maps.
In this thesis, the proposed process of estimation of NSSR has proven that, eliminates the need for ancillary ground data to produce solar radiation data as well as identified need of spatially distributed input parameters such as water vapour content.
To estimate the diurnal variations of NSSR, a sinusoidal model has proposed and this sinusoidal model is capable of retrieving the diurnal variation of NSSR for clear sky and cloudy skies. Therefore this model can apply without separating cloudy or clear sky conditions and the model estimate solar radiation for all sky conditions in reasonable accuracy.
Estimation of NSSR for clear sky has shown better performance than cloudy sky condition.
Cloudy sky conditions make estimating NSSR from satellite data difficult. Therefore, cloudy-sky estimation have shown the higher RMSE than clear sky.
The proposed method in this research for estimation of DANR, compared to other methods, no need of sun rise and sun set time to have DANR. Accurate day length increases the estimated accuracy of DANR. Another immense advantage of the suggested method is that it has greater spatial coverage compared to available acrylic data and provide greater opportunity for user community in solar radiation map users.

MODIS Terra day overpasses images and products based retrieval from remote sensing data as input to acquire the instantaneous NSSR at 1 km resolution. Ground observation from one station in Iran and one station from Penn State USA were selected to validate the accuracy and performance of this model for different seasons in different sky conditions.
Model validation in different seasons was interesting, to check the model accuracy and test the model performances. The results of model validation in Penn State, USA with SURFRAD data shows larger RMSE values compared to the instantaneous NSSR in Tehran Province. However, the validation results indicated in Chapter 8, mentioned that similar results have obtain by different researches in same location with SURFRAD data. The daily average values constructed from the MODIS Terra and agreed well with ground measured data.

This model can apply for clear skies as well as cloudy sky conditions as described in Chapter 7. All products estimated by method originated in this study have a 1 km spatial resolution and comparable accuracy in pixel level. Comparison with estimated DANR with previous results was difficult, because no sources reported performances for DANR calculation using this model.

It is an important to study and, enumerates several sources of error that may affect operational estimation and implementation of proposed NSSR estimation model from MODIS data and products. Errors caused by uncertainties of satellite retrievals for different atmospheric conditions in different surfaces to be considered. Spatially distributed process models are becoming widely used, for solar radiation estimation in global scale. Hence, for environmental modelling, it is suitable to measure the model uncertainties and provide not only point estimates for output variables but also confidence intervals as well, because atmospheric uncertainties always associating with remotely sensing products.

MODIS satellite images, used in this thesis as well provide more data and products for large areas and this model does not require ancillary data to estimate NSSR. Therefore the spatial resolution of raw input MODIS data can be retained. The spatial resolution of the MODIS remotely sensed data supported and to be extended to analysis the trend of present solar radiation estimation in the existing metrological based observations.
In addition, up-scaling from ground point observations to the MODIS spatial resolution, using higher resolution remotely sensed data is proposed because ground point observations have not be sufficient to validate the estimated measurements at MODIS resolutions. This would be badly affected in large area as well as heterogeneous areas. Better solution for control of such kind of situation is to produce sufficient number of point observations during the satellite overpass time in relevant areas.

However, it has noted that in this research selected bands in MODIS detectors, have enough information to influence estimated solar radiation such as clouds, water vapours, sensor zenith angle, and solar zenith angle etc. There are other products from MODIS images such as aerosol and gases etc. That will be able to improve the model in further to have more accurate estimations.
Comparison with existing methods, this research achieved expected targets as proposed in the beginning in our problem statement and research questions.

9.2. Recomendations

MODIS terra satellite is a multi-spectral sensor, acquiring data in 36 spectral bands and provide their products with an opportunity to retrieve surface shortwave radiation accurately. Furthermore, many atmospheric and land parameters have been produced as standard products and are easy to obtain and process without any technical disturbances. Based on MODIS products, our developed and proposed model has performs better in different locations as well as different seasons in clear and cloudy conditions. However, the quality of MODIS products can produce large errors in the estimation of NSSR due to atmospheric interaction. Therefore, to further improve the accuracy of estimation of solar radiation derived from MODIS products, some outstanding issues need to be addressed.

Hence, following points to be noted in further investigation and this approach will gives greater flexibility to improve the existing model performances.

An extended error analysis needs to be carried out to identify the major error and error sources of MODIS data as well as implemented model. To do this a good record of ground observation network and field measurements of specific, well-characterized sites are critical in order to develop a model for estimating the net surface shortwave solar radiation and to developing an understanding of parameters involved in the estimation.

Terra MODIS instrument image the entire Earth's surface every one to two days, such a temporal resolution solar radiation data from MODIS can be instrumental in validating other remote sensing data products in remote regions where ground observations are not available. At the same time. The results from this study appear to be comparable or better to currently available NSSR estimation methodology that uses ancillary ground based observations.

The model results were based on comparison with ground observations, while assuming that the ground measured solar radiation represent the same sample spatial scale (1 km x 1 km) as that of the MODIS derived value. This assumption could lead to large discrepancies when ground stations are not maintaining well. Hence, one strategy would be to improve the quality of ground station instruments.

It has explicitly recognized that the need of spatially varied parameters to perform model well, the future research work would oriented for retrieved NSSR or its components by selecting of satellite images or its products for atmospheric parameter selections. Therefore the most straightforward way of using proper analysis method of selecting satellite images and their products. Then such a proper approach does not allow to decrees the model performances.

It has noted that there is no computational or technical limitation to apply this model to finer satellite data than 1 km, however, consideration on space and time mismatch and atmospheric heterogeneity issue (clouds contamination) should be considered. In addition, to improve the temporal resolution of estimated solar radiation, accurate daily average NSSR can be estimated by using the two MODIS observations from Terra and Aqua.in one day.

ACRONYMS

α:	Land surface reflectance (or albedo)
e_0 :	Vapour pressure
λ:	Waveband of the channel
TOA:	Top of the atmosphere
Rn:	Net radiation
RS ↓:	Downward shortwave radiation
RS ↑:	Upward shortwave radiation
RL ↓:	Downward long-wave radiation
RL ↑:	Upward long-wave radiation
σ:	Stefan-Boltzmann constant
S_0 :	Solar constant at the mean Earth-Sun distance
SZA:	Solar zenith angle
δ:	Solar declination of the Sun
φ:	Geographic latitude
ω:	Solar hour angle
E_0:	TOA solar irradiance at one astronomical unit (1.369 kW/m²)
d_L:	Earth–Sun distance in astronomical units
M	cosine of the solar zenith angle
r'	TOA broadband albedo
r	Earth Radius
F_u:	Upwards flux at the TOA
w_e:	precipitable water vapour

LIST OF REFERENCES

Aaron., D., & David, S. B. (2011). Atmospheric and Surface Contributions to Planetary Albedo. *Journal of Climate and Applied Meteorology, 24*, 4402-4418.

Ackerman, S., Strabala, K., Menzel, P., Frey, R., Moeller, C., Gumley, L., Zhang, H. (2006). Discriminating Clear Sky From Cloude With MODIS Algoritham Therotical Basics Document (MOD35). *NASA, LaRC, Hampton, VA*.

Ahmad, S. P., V. V. Salomonson, W. L. Barnes, X. Xiong, G. G. Leptoukh, & G. N. Serafino. (2002). MODIS Radiances and Reflatances for Earth System Science Studies and Environmental Applications. . NASA/GSFC, Code 902, Greenbelt, MD 20771.

Bennett, N. D., Croke, B. F. W., Guariso, G., Guillaume, J. H. A., Hamilton, S. H., Jakeman, A. J., Andreassian, V. (2013). Characterising performance of environmental models. *Environmental Modelling & Software, 40*(0), 1-20.

Bisht, G., & Bras, R. L. (2010). Estimation of net radiation from the MODIS data under all sky conditions: Southern Great Plains case study. *Remote Sensing of Environment, 114*(7), 1522-1534.

Bisht, G., & Bras, R. L. (2011). Estimation of Net Radiation From the Moderate Resolution Imaging Spectroradiometer Over the Continental United States. *Geoscience and Remote Sensing, IEEE Transactions on, 49*(6), 2448-2462.

Bisht, G., Venturini, V., Islam, S., & Jiang, L. (2005). Estimation of the net radiation using MODIS (Moderate Resolution Imaging Spectroradiometer) data for clear sky days. *Remote Sensing of Environment, 97*(1), 52-67.

Bojanowski, J. S. (2013). Calibration of solar radiation models for Europe using Meteosat Second Generation and weather station data, (MSc thesis, ITC).

Brutsaert, W. (1975). On a derivable formula for long-wave radiation from clear skies. *Water Resources Research, 11*(5), 742-744.

Cano, R., Pinker, R. T., Kustas, W. P., Laszlo, I., Moran, M. S., & Huete, A. R. (1994). Basin-scale solar irradiance estimates in semiarid regions using GOES 7. *Water Resources Research, 30*, 1375-1386.

Cano., D., Monget, J. M., Albuisson, M., Guillard, H., & Wald, L. (1986). A method for the determination of the global solar-radiation from meteorological satellite data, . *Solar Energy, 37*, 31 - 39.

Cebecauer, T., Suri M., & Gueymard C. (2011). *Uncertainty sources in satellite-derived Direct Normal Irradiance: How can prediction accuracy be improved globally.* Paper presented at the Proceedings of the SolarPACES Conference, Granada, Spain.

Cess, R. D., Dutton, E. G., Deluisi, J. J., & Jiang, F. (1991). Determining Surface Solar Absorption from Broadband Satellite Measurements for Clear Skies: Comparison with Surface Measurements. *Journal of Climate, 4*(2), 236-247.

Cess, R. D., & Vulis, I. L. (1989). Inferring Surface Solar Absorption from Broadband Satellite Measurements. *Journal of Climate, 2*(9), 974-985.

Dedieu, G., Deschamps, P. Y., & Kerr, Y. H. (1987). Satellite Estimation of Solar Irradiance at the Surface of the Earth and of Surface Albedo Using a Physical Model Applied to Metcosat Data. *Journal of Climate and Applied Meteorology, 26*(1), 79-87.

Dekker, J., Nthontho, M., Chowdhury, S., & Chowdhury, S. P. (2012). Investigating the effects of solar modelling using different solar irradiation data sets and sources within South Africa. *Solar Energy, Volume 86*(9), 2354-2365.

Diak, G. R., & Whipple, M., S,. (1993). Improvements to models and methods for evaluating the land-surface energy balance and effective roughness using radiosonde reports and satellite-measured skin temperature data. *Agricul. and Forest Meteorol, 63 no 3-4*, 189-218.

Duguay, C. R. (1995). An approach to the estimation of surface net radiation in mountain areas using remote sensing and digital terrain data. *Theoretical and Applied Climatology, 52*(1-2), 55-68.

Gao, B. C., & Kaufman, Y. J. (1990). The MODIS Near-IR Water Vapor Algorithm, MOD05, Total Precipitable Water. *Climate and Radiation Branch, NASA Goddard Space Flight Center Greenbelt, MD 20771*.

Gautier, C., Diak, G., & Masse, S. (1980). A simple model to estimate the incident solar radiation at the surface from GOES satellite data. *Journal of Applied Meteorology, 19*, 1005-1012.

Gautier, C., & LandSfield, M. (1997). Surface solar radiation flux and radiative forcing for the Atmospheric Radiation Measurement (ARM) Southern Great Plains (SGP): A satellite, surface observations, and radiative transfer model study. *Journal of Atmospheric Sciences, 54*, 1289-1307.

Guenther, B., Godden, G. D., Xiong, X. X., Knight, E. J., Qiu, S. Y., Montgomery, H., Hao, Z. D. (1998). Prelaunch algorithm and data format for the Level 1 calibration products for the EOS-AM1 Moderate Resolution Imaging Spectroradiometer (MODIS). *Ieee Transactions on Geoscience and Remote Sensing, 36*(4), 1142-1151.

Hahmann, A. N., D. M. Ward, & R. E. Dickinson. (1995). Land surface temperature and radiative fluxes response of the NCAR CCM2/Biosphere-Atmosphere Transfer Scheme to modifications in the optical properties of clouds. *Journal of Geophysics Resources, 100*, 23239-23252.

Hamon, R. W., Weiss, L. L., & Wilson, W. T. (1954). Insolation as an emperical function of daily sunshine duration. *Monthly Weather Review, 82*(6), 141-146.

Houborg, R., Soegaard, H., W.Emmerich, & Moran, S. (2007). Inferences of all-sky solar irradiance using Terra and Aqua MODIS satellite data. *International Journal of Remote Sensing, Vol. 28, No. 20*, 4509–4535.

Huang, G., Liu, S., & Liang, S. (2012). Estimation of net surface shortwave radiation from MODIS data. *International Journal of Remote Sensing, 33*(3), 804-825.

Hwang, K., Choi, M., Lee, S., & Seo, J. (2012). Estimation of instantaneous and daily net radiation from MODIS data under clear sky conditions: a case study in East Asia. *Irrigation Science*, 1-12.

Iqbal, M. (1983). *An Instroduction to Solar Radiation*: Acadamic Press.

ISO-1960:1990. Solar Energy-Specification and Classification of Instruments for Measuring Hemispherical Solar and Direct Solar Radiation.

ISO-9847:1993. Solar Energy- Calibration of field pyranometers by comparison to a reference pyranometer.

Janjai, S. (2010). A method for estimating direct normal solar irradiation fromsatellite data for a tropical environment. *Solar Energy, 84*, 1685-1695.

John, A., John J. DeLuisi, & Long, C. N. (2000). SURFRAD—A National Surface Radiation Budget Network for Atmospheric Research. *Bulletin of the American Meteorological Society*.

Kato, S., Fred G. Rose, David A. Rutan, & Thomas P. Charlock. (2007). Cloud Effects on Meridional Atmospheric Energy Budget Estimated from Clouds and the Earth's Radiant Energy System (CERES) Data. *Journal of Climate*.

Kaufman., J. Y., & Didier., T. (1998). Algorithms for Remote Sensing of Topospheric Aerosol from MODIS. MODIS-ATDB.

Keunchang., J., Sinkyu., K., & Joon., K. (2010). Estimation of Net Radiation using MODIS under All Sky Conditions. KNU, Dept. of Environmental Science.

Kim, H. Y., & Liang, S. (2010). Development of a hybrid method for estimating land surface shortwave net radiation from MODIS data. *Remote Sensing of Environment, 114*(11), 2393-2402.

Kim., H. Y. (2008). *Estimation of Land Surface Radiation Budget from MODIS Data.* (Doctor of Philosophy), University of Maryland, Faculty of the Graduate School.

Lagouarde, J. P., & Brunet, Y. (1993). A simple model for estimating the daily upward longwave surface radiation flux from NOAA-AVHRR data. *International Journal of Remote Sensing, a4(5)*, 907-925.

Li, Z., Leighton, H. G., Masuda, K., & Takashima, T. (1993a). Estimation of SW Flux Absorbed at the Surface from TOA Reflected Flux. *Journal of Climate, 6*(2), 317-330.

Li., Z., Leighton, H. G., & Cess, R. D. (1993b). Surface net solar radiation estimated from satellite measurements: Comparisons with tower observations. *Journal of Climate, Vol. 6*, 1764−1772.

Liang, S. (2004). *Quantitative remote sensing of land surfaces*. Hoboken, NJ: Wiley: University of Toronto Press

Liang, S., Xiaowen Li, & Jindi Wang. (2012). *Advanced Remote Sensing*: Academic Press is an imprint of Elsevier.

Liang., S., Zheng, T., Liu, R. G., Fang, H., Tsay, S. C.,, & Running, S. (2006). Estimation of incident photosynthetically active radiation from Moderate Resolution Imaging Spectrometer data. *Journal of Geophysical ResearchAtmospheres, 111, D15208*.

Masuda, K., Leighton, H. G., & Li, Z. (1995). A New Parameterization for the Determination of Solar Flux Absorbed at the Surface from Satellite Measurements. *Journal of Climate, 8*(6), 1615-1629.

Michale, D. K., Steven Platnic, & Menghua Wang. (1997). Cloud Retrieval Algorithms for MODIS: Optical Thickness, Effective Particle Radius, and Thermodynamic Phase *MODIS Algorithm Theoretical Basis Document No. ATBD-MOD-05, MOD06 – Cloud product*: NASA Goddard Space Flight Center.

Morris, M. D. (1991). Factorial Sampling Plans for Preliminary Computational Experiments. *Technometrics, 33*, 161-174.

Nightingale, J. M., Morisette, J. T., Wolfe, R. E., Tan, B., Gao, F., Ederer, G., Turner, D. P. (2009). Temporally smoothed and gap-filled MODIS land products for carbon modelling: application of the fPAR product. *International Journal of Remote Sensing, 30*(4), 1083-1090.

Noia, M., C. F. Ratto, & R. Festa. (1993). Solar Irradiance Estimation from geostationary Stellite Data. *Solar Energy, 05, No: 06*, 449-456.

Pinker, & Ewing, J. A. (1985). Modeling Surface Solar Radiation: Model Formulation and Validation. *Journal of Climate and Applied Meteorology, 24*(5), 389-401.

Pinker, R.Rrouin, & Z.Li. (1995). A Review of Satellite Methods to Derive Surface Shortwave Irradiance. *Remote Sensing of Environment*, 108-124.

Qin, J., Chen, Z., Yang, K., Liang, S., & Tang, W. (2011). Estimation of monthly-mean daily global solar radiation based on MODIS and TRMM products. *Applied Energy, 88*(7), 2480-2489.

Rebecca, L., & David, H. (2000). NASA's Earth observing System. Goddard Space Flight Center, Maryland, 20771.

Rigollier, C., M., L., & Wald L. (2004). The method Helosat 2 for deriving shortwave solar radiation from satellite images. *Solar Energy 77, 2*, 159-169.
Roerink, G. J., Bojanowski, J. S., de Wit, A. J. W., Eerens, H., Supit, I., Leo, O., & Boogaard, H. L. (2012). Evaluation of MSG-derived global radiation estimates for application in a regional crop model. *Agricultural and Forest Meteorology, 160*(0), 36-47.
Saltelli, A., S. Tarantola, & Campolongo., F. (2000). Sensitivity analysis as an ingredient of modelling *Statistical Science, 15(4)*, 377-395.
Schillings, C., Mannstein, H., & Meyer, R. (2004). Operational method for deriving high resolution direct normal irradiance from satellite data. *Solar Energy, 76*, 475–484.
Shunlin, L., Kaicun, W., Xiaotong, Z., & Wild, M. (2010). Review on Estimation of Land Surface Radiation and Energy Budgets From Ground Measurement, Remote Sensing and Model Simulations. *IEEE Journal of Selected Topics in Applied Earth Observations and Remote Sensing, 3*(3), 225-240.
Sridhar, V., & Elliott, R. L. (2002). short communication On the development of a simple downwelling longwave radiation scheme. *Agricultural and Forest Meteorology, 112*, 237-243.
Tang, B., Zhao, L. L., & Renhua Zhang. (2006). A direct method for estimating net surface shortwave radiation from MODIS data. *Remote Sensing of Environment*, 115-126.
Tarpley, J. D. (1979). Estimating Incident Solar Radiation at the Surface from Geostationary Satellite Data. *Journal of Applied Meteorology, 18*(9), 1172-1181.
Tianxing, W., Yan, G., & Chen, L. (2012). Consistent retrieval methods to estimate land surface shortwave and longwave radiative flux components under clear-sky conditions. *Remote Sensing of Environment, 124*, 61-71.
Todd, A., Schroeder, Robbie Hember, Nicholas, & C, C. (2009). Validation of Solar Radiation Surfaces from MODIS and Reanalysis Data over Topographically Complex Terrain. *Journal of Applied Meterology and Climatology, 48*, 2441-2458.
Toller, G. N., Isaacman, A., Kuyper, J., & Salomonson, V. (2006). MODIS Level 1B Product User's Guide. *NASA/Goddard Space Flight Center*.
Tugjsuren, N., & Batbayar, J. (2011). *Shortwave radiation estimation from Modis-terra data over semi-arid region in mongolia.* Paper presented at the 2011 6th International Forum.
URL-1. http://eospso.gsfc.nasa.gov/.
URL-2. http://ladsweb.nasacom.nasa.gov/.
URL-3. http://www.timeanddate.com/information/.
URL-4. ftp://aftp.cmdl.noaa.gov/data/radiation/surfrad/.
Wan, Z. (1999). *MODIS Land-Surface Temperature Algorithm Theoretical Basis Document (LSt-ATDB).* Paper presented at the International Land-Surface Temperature Workshop, University of California at Santa Barbara, CA.
Wang, & Liang., S. (2009). Estimation of high-spatial resolution clear-sky longwave downward and net radiation over land surfaces from MODIS data. *Remote Sensing of Environment, 113*(4), 745-754.
Wang, & Pinker, R., T,. (2009). Shortwave radiative fluxes from MODIS: Model development and implementation. *Journal of Geophysical Research: Atmospheres, 114*(D20), D20201.
Wang, Zhengming, W., Pucai Wang, Michael Sparrow, Jingmiao Liu, Xiuji Zhou, & Shigenori, H. (2005). Estimation of surface long wave radiation and broadband emissivity using Moderate Resolution Imaging Spectroradiometer (MODIS) land surface temperature/emissivity products. *Journal of Geographical Research, 110*, D11109.
White, G. H., E. Kalnay, R. Gardner, & M. Kanamitsu. (1993). The skill of precipitation and surface temperature forecasts by the NMC global model during DERF II. *Monthly Weather Review, 121*, 805-814.
William., F., Edward J. Rykiel, Randal S. Stahl, Hsin-i Wu, & Robert M. Schoolfield. (1995). A model comparison for daylength as a function of latitude and day of year. *Ecological Modelling, 80*, 87-95.
WMO. (2008). *Guide to Meteorological Instruments and Methods of Observation* (Vol. WMO-No. 8). Switzerland World Meteorological Organization.
Zelenka, A., Perez, R., Seals, R., & Renné, D. (1999). Effective Accuracy of Satellite-Derived Hourly Irradiances. *Theoretical and Applied Climatology, 62*(3-4), 199-207.

APPENDIX

Appendix 1: MODIS spectral band specifications.

Primary Use	Band number	Central wavelength [nm]	Bandwidth[nm]	Spatial resolution [m]
Land / Cloud / Aerosols / Boundaries	1	645	620 -670	250
	2	858.5	841 -876	
Land / Cloud / Aerosols Properties	3	469	459 -479	500
	4	555	545 -565	
	5	1240	1230 -1250	
	6	1640	1628 -1652	
	7	2130	2105 -2155	
Ocean Color / Phytoplankton/ Biogeochemistry	8	421.5	405 -420	1000
	9	443	438 -448	
	10	488	483 -493	
	11	531	526 -536	
	12	551	546 -556	
	13	667	662 -672	
	14	678	673 -683	
	15	748	743 -753	
	16	869.5	862 -877	
Atmospheric Water Vapor	17	905	890 -920	
	18	936	931 -941	
	19	940	915 -965	
Surface / Cloud Temperature	20	3750	3660 -3840	
	21	3959	3929 -3989	
	22	3959	3929 -3989	
	23	4050	4020 -4080	
Atmospheric Temperature	24	4465.5	4433 -4498	
	25	4515.5	4482 -4549	
Cirrus Clouds / Water Vapor	26	1375	1360 -1390	
	27	6715	6535 -6895	
	28	7325	7175 -7475	
Cloud Properties	29	8550	8400 -8700	
Ozone	30	9730	9580 -9880	
Surface / Cloud Temperature	31	11030	10780 -11280	
	32	12020	11770 -12270	
Cloud Top Altitude	33	13335	13185 -13485	
	34	13635	13485 -13785	
	35	13935	13785 -14085	
	36	14235	14085 -14385	

(Source: http://modis.gsfc.nasa.gov/about/specifications.php)

Appendix 2: Coefficient of the TOA narrowband to broadband conversion for different solar zenith angles in forward direction.

SZA		b_0	b_1	b_2	b_3	b_4	b_5	b_6	b_7
0	C_1	-0.05403	0.84088	0.18487	1.40413	-1.64202	0.19707	-0.03715	0.16918
	C_2	0.02036	2.49949	0.34567	2.88350	-5.60429	-1.30626	0.39343	-0.56029
	C_3	1.73271	0.17257	1.19778	-0.02851	-0.04349	-0.22705	0.78731	0.45516
	C_4	0.16932	0.34613	0.70489	0.51796	0.53910	1.09412	0.35910	0.27905
10	C_1	-0.05393	0.81169	0.09114	1.37593	-1.59514	0.19221	-0.01136	0.14783
	C_2	0.03405	2.38133	1.10520	3.22075	-5.39629	-2.10978	0.15091	-0.05062
	C_3	1.74286	0.18870	-0.08161	-0.03073	0.00410	-0.52258	1.17408	1.14425
	C_4	0.33363	0.34667	1.05425	0.49437	0.52550	0.89482	0.22749	0.11623
20	C_1	-0.04717	0.78668	0.11821	1.36837	-1.58457	0.18723	-0.02421	0.12043
	C_2	0.03211	2.64369	0.98016	8.78781	-11.52053	-2.48273	0.31381	0.20507
	C_3	1.73526	0.20550	0.46313	-0.31940	-0.30227	-0.39247	-0.08602	-0.07858
	C_4	0.29155	0.32646	0.62314	0.41361	0.47238	0.75225	0.99147	0.59902
30	C_1	-0.06510	0.75695	0.09025	1.31840	-1.52716	0.16408	0.02624	0.06195
	C_2	0.07563	2.38618	0.73612	3.95866	-5.63249	-2.01480	0.66823	0.29240
	C_3	1.72955	0.23451	0.80797	-0.00547	0.06709	0.02937	0.37354	-0.86485
	C_4	0.60936	0.32285	0.59212	0.44557	0.47552	0.60948	0.31681	1.69123
40	C_1	-0.04840	0.73721	0.09098	1.29230	-1.50695	0.14319	0.07579	0.04049
	C_2	0.04656	1.77321	2.42373	3.73010	-3.92107	-4.22008	0.70597	0.39034
	C_3	1.70345	0.27161	0.26188	0.01101	0.27028	-0.02978	0.04214	-0.47093
	C_4	0.26552	0.33291	0.42813	0.43821	0.44650	0.43587	0.37154	0.81975
50	C_1	-0.05594	0.69302	0.04902	1.26768	-1.47995	0.16009	0.12810	0.00691
	C_2	0.06018	1.37413	6.66617	3.18884	-2.96946	-4.14039	0.06120	0.03508
	C_3	1.68794	0.56141	-0.26487	0.07170	0.47417	-0.04511	1.32410	1.86992
	C_4	0.23031	0.24758	0.48945	0.41208	0.38074	0.49672	0.04246	0.14504
60	C_1	-0.08365	0.52101	0.20470	1.17619	-1.31026	-0.00664	0.13764	0.04693
	C_2	0.12443	3.76866	6.82781	3.00476	-3.89719	-3.82384	0.24585	-0.75481
	C_3	1.60598	0.30130	-0.18111	0.06978	0.41114	0.03775	1.17798	0.65163
	C_4	0.32150	0.32131	0.40112	0.42072	0.38700	0.42230	0.16340	0.24966
70	C_1	-0.14794	0.23680	0.24933	1.00386	-1.00917	-0.20956	0.12883	0.09424
	C_2	0.27048	6.26712	1.12753	3.24162	-3.05223	-1.46739	3.52008	-3.26873
	C_3	1.55063	0.27384	-0.86731	0.26817	0.71117	-0.31201	0.27741	0.37701
	C_4	0.46241	0.34113	1.70942	0.35020	0.33393	0.70404	0.33812	0.31917